frontiers | Frontiers in Marine Science

TYPE Review
PUBLISHED 02 April 2024
DOI 10.3389/fmars.2024.1331164

OPEN ACCESS

EDITED BY
Marco Ghisalberti,
University of Western Australia, Australia

REVIEWED BY
Jeff Shimeta,
RMIT University, Australia
Karly Cohen,
University of Florida, United States

*CORRESPONDENCE
S. Laurie Sanderson
slsand@wm.edu

RECEIVED 31 October 2023
ACCEPTED 15 March 2024
PUBLISHED 02 April 2024

CITATION
Sanderson SL (2024) Particle separation mechanisms in suspension-feeding fishes: key questions and future directions.
Front. Mar. Sci. 11:1331164.
doi: 10.3389/fmars.2024.1331164

Particle separation mechanisms in suspension-feeding fishes: key questions and future directions

S. Laurie Sanderson*

Department of Biology, William & Mary, Williamsburg, VA, United States

Key unresolved questions about particle separation mechanisms in suspension-feeding fishes are identified and discussed, focusing on areas with the potential for substantial future discovery. The published hypotheses that are explored have broad applicability to biological filtration and bioinspired improvements in commercial and industrial crossflow microfiltration processes and microfluidics. As the first synthesis of the primary literature on the particle separation mechanisms of marine, estuarine, and freshwater suspension-feeding fishes, the goals are to enable comparisons with invertebrate suspension-feeding processes, stimulate future theoretical and empirical studies, and further the development of biomimetic physical and computational fluid dynamics models. Of the eight particle separation mechanisms in suspension-feeding fishes, six have been proposed within the past twenty years (inertial lift and shear-induced migration, reduction of effective gap size by vortices, cross-step filtration, vortical flow along outer faces of gill raker plates, ricochet filtration, and lateral displacement). The pace of discovery is anticipated to continue accelerating. Multidisciplinary collaboration and integration among biologists and engineers (including chemical, mechanical, biomedical, and filtration engineering) will result in new perspectives to identify patterns and potential unifying mechanisms across the breadth of suspension-feeding fish taxa, morphology, and function.

KEYWORDS

suspension feeding, filter feeding, particle separation, gill rakers, crossflow filtration, microfiltration, inertial microfluidics, lateral displacement arrays

1 Introduction

Suspension-feeding (SF) fishes are of substantial ecological and economic importance. Because they feed on small suspended particles such as phytoplankton, zooplankton, and detritus but serve as prey for larger predatory fish, birds, and mammals, SF fishes are key components of marine and freshwater food webs. Approximately 25% of the annual global fish harvest is composed of SF fishes (FAO, 2021). SF fish species have been subjects of recent concern regarding microplastics in the food chain (e.g., Savoca et al., 2020; Misic et al., 2022).

Biomanipulation to improve the quality of inland waters has involved the introduction or the removal of SF fishes (review in Lürling and Mucci, 2020). In addition, biomimetic and bioinspired solutions for separation technology and water filtration are topics of intense current interest (Goel et al., 2021; Bianciardi and Cascini, 2022; Hamann and Blanke, 2022; Zhang et al., 2022b). Recent discoveries of particle separation mechanisms in SF fishes have stimulated the development of biomimetic models with potential applications in microfluidics and commercial and industrial filtration for foods and beverages, wastewater, irrigation, oil spill remediation, and biotechnology products (e.g., Dou et al., 2017; Schroeder et al., 2019; Clark and San-Miguel, 2021; Adelmann et al., 2022; Masselter et al., 2023; Xu et al., 2023).

The application of industrial aerosol filtration theory to biological hydrosol filtration (Rubenstein and Koehl, 1977) and the development of particle encounter rate models in aquatic ecosystems (Shimeta and Jumars, 1991; Espinosa-Gayosso et al., 2021) provide a valuable framework for mechanistic studies of suspension feeding. As established by Shimeta and Jumars (1991), particle encounter (i.e, "initial contact of the particle and the feeding structure, regardless of retention") is distinct conceptually from particle capture. Inertial impaction and/or direct interception have been identified as particle encounter mechanisms in SF fishes (e.g., Sanderson et al., 1996b; Paig-Tran et al., 2011; Divi et al., 2018; Witkop et al., 2023). Rather than reviewing these particle encounter mechanisms that result in the initial contact between the particle and the filter element, this article focuses on a comprehensive analysis of particle separation mechanisms that could result in the concentration of particles within the oral cavity, including sieving, mucus entrapment, inertial lift and shear-induced migration, reduction of effective gap size by vortices, cross-step filtration, vortical flow along outer faces of gill raker plates, ricochet filtration, and lateral displacement. The functional morphology, biomechanics, and fluid dynamic processes that cause particles to interact with the filter elements in SF fishes will be examined, and key questions and research priorities will be identified and discussed.

1.1 Scope and diversity of SF fishes

Suspension feeding can be defined as the separation of small suspended particles from volumes of water, involving both microphagy and planktivory (Jørgensen, 1966; Sanderson and Wassersug, 1993). Fish suspension feeding refers here to feeding on suspended prey ranging from single-celled bacteria and microalgae (~ 5 μm diameter) to planktonic crustaceans (~ 5 mm length) that are too small to be sensed and consumed individually (Lazarro, 1987; Sanderson and Wassersug, 1993; Gerking, 1994). Because size is relative, a whale shark with a total length of 6 m can consume multiple small fishes during SF, along with planktonic crustaceans and fish eggs (Motta et al., 2010).

Detritivorous fish species, including microphagous benthic feeders that filter edible particles from sediment suspended inside the oral cavity during a process referred to as winnowing (e.g., Weller et al., 2017; Brodnicke et al., 2022), could also be studied from the perspective of particle separation mechanisms. In contrast, fish particulate feeding involves targeting and consuming larger planktonic prey individually. However, many SF fish species are facultative suspension feeders that also use particulate feeding to consume larger prey individually, and criteria for distinguishing between suspension feeding and particulate feeding have not been established among species (Hamann et al., 2023).

SF fishes include familiar species such as goldfish and carp (Cyprinidae), menhaden (Clupeidae), paddlefish (Polyodontidae), manta and devil rays (Mobulidae), the whale shark (Rhincodontidae) and basking shark (Cetorhinidae), a number of mackerel species (Scombridae), and many tilapia (Cichlidae), herring (Clupeidae), and anchovy (Engraulidae) (Figure 1). There are as many as 21 families of SF fishes in 12 orders (Cheer et al., 2012). Sanderson and Wassersug (1993) provided a comprehensive summary on the pump and ram SF fish species from the primary literature. That list of approximately 50 species has not been updated, and there are now more than 100 additional SF fish species reported in the literature.

1.2 Anatomical framework

The filter of SF fishes consists of a network of filter elements enclosed inside the mouth, typically termed the branchial arches, gill rakers, and associated protrusions (Figure 2). The morphology of the filter elements can change substantially during ontogeny (e.g., Cohen and Hernandez, 2018). The term oral cavity will be used to refer to the entire buccal cavity and pharyngeal cavity of fishes, also called the buccopharyngeal, oropharyngeal, or orobranchial cavity. The oral cavity of most extant osteichthyan fishes and elasmobranchs has five pairs of branchial arches (BAs), also referred to as gill arches or pharyngeal arches (Nelson, 1967a; Wegner, 2015). While there is substantial variability among orders and families, in general each of the anterior five BAs has a row of bony or cartilaginous protuberances called gill rakers (GRs) on the anterolateral side of each BA. In addition, many fish species also have a row of GRs on the posteromedial side of each BA. The keratinized GRs of basking sharks (*Cetorhinus maximus*) lack epithelial tissue (Paig-Tran and Summers, 2014).

The GRs frequently have protrusions on their surfaces which can be rounded or spiny and which may be unnamed or may be termed "denticles", "branchiospinules", or "teeth" depending on the taxon and the author (e.g., "Filter Element" in Table 1 and "Dimension Measured" in Table 2). Because the genetic, developmental, and evolutionary origins of these protrusions on the gill rakers have not been studied, potential relationships between these protrusions and odontodes, oral teeth, and dermal denticles are not known (Paig-Tran and Summers, 2014; Mori and Nakamura, 2022; Cooper et al., 2023). In general, the BAs, GRs, and associated protrusions have an epithelial tissue layer with multiple cell types that can include mucus-secreting cells and taste buds (Sanderson and Wassersug, 1993).

There is no evidence that fish swallow a notable volume of water at the esophagus during SF (Provini et al., 2022). Flow that enters the mouth during SF passes between the GRs and their associated

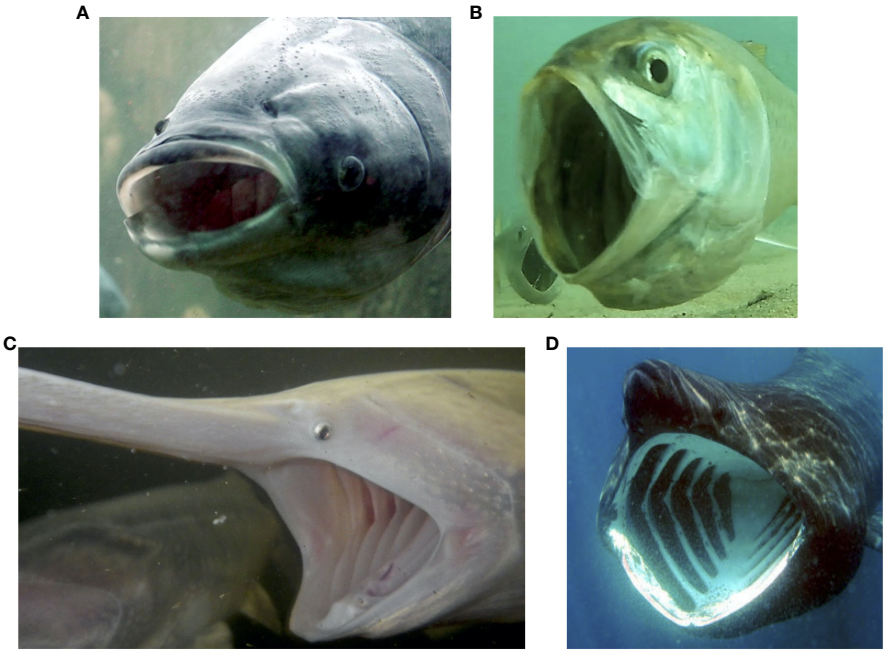

FIGURE 1
Examples of SF fish species belonging to four orders, shown during SF. **(A)** Pump SF bighead carp, *Hypophthalmichthys nobilis*, Cyprinidae, Cypriniformes. © Solomon David, used with permission, not covered by the CC BY license. **(B)** Ram SF Atlantic menhaden, *Brevoortia tyrannus*, Clupeidae, Clupeiformes. © myfishingcapecod.com, used with permission, not covered by the CC BY license. **(C)** Ram SF American paddlefish, *Polyodon spathula*, Polyodontidae, Acipenseriformes. Rob Helm, USFWS https://www.flickr.com/photos/usfwsmtnprairie/9546645557/ CC BY 2.0 https://creativecommons.org/licenses/by/2.0/ **(D)** Ram SF basking shark, *Cetorhinus maximus*, Cetorhinidae, Lamniformes. jidanchaomian https://www.flickr.com/photos/10565417@N03/6246022639, CC BY-SA 2.0 https://creativecommons.org/licenses/by-sa/2.0/.

protrusions to exit from the oral cavity into the opercular cavities (also called the branchial cavities in osteichthyan fishes) or parabranchial cavities (in elasmobranchs). In the opercular cavities, the gill filaments where gas exchange occurs are attached to the aboral (i.e., external) surfaces of the BAs. After traveling across the gill filaments, the water exits from the opercular cavities on the ventral and/or lateral sides of the head by passing beneath the bony operculum. Thus, in all SF fishes, water exits from the oral

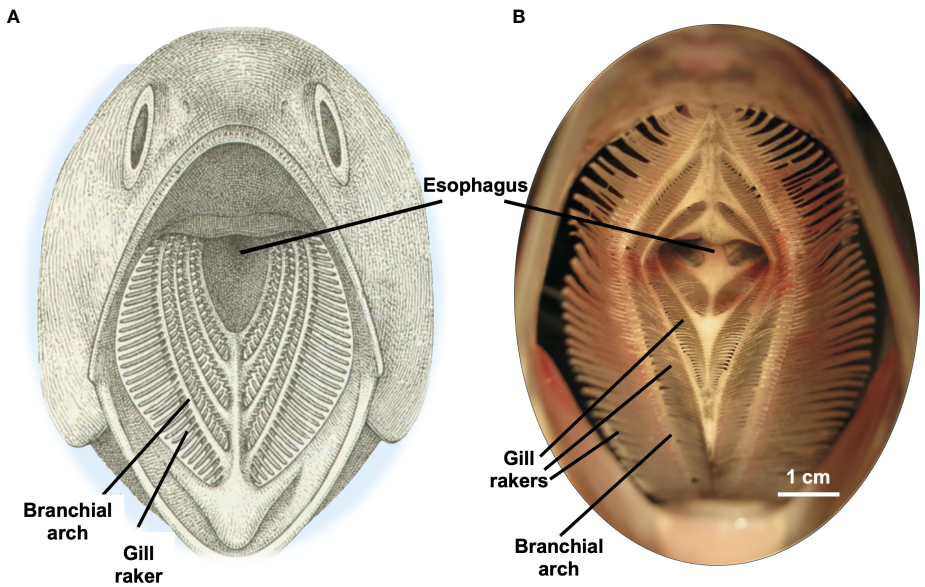

FIGURE 2
Examples of SF fish oral cavities shown in frontal view, illustrating branchial arches with gill rakers extending laterally from each branchial arch. **(A)** Generalized SF fish. Modified from Sanderson and Wassersug (1990), with permission. **(B)** American shad, *Alosa sapidissima*, Clupeidae. Modified from Witkop et al. (2023), CC BY 4.0.

TABLE 1 Compilation of reported Reynolds numbers (Re) that have been calculated at the level of the proposed filter elements in suspension-feeding (SF) fishes.

Family	Species	Common Name	Pump or Ram	Body Size	Filter Element	Filter Element Size	Flow Speed	Re	Reference
Cichlidae	*Oreochromis esculentus*	Ngege (Singida) tilapia	Pump	26 cm SL	Gill raker	250 - 1500 µm width	35 - 70 cm s^{-1}	150 - 600	Sanderson et al., 2001
Clupeidae	*Alosa sapidissima*	American shad	Ram	38 - 41 cm SL	Gill raker	1000 µm height	45 cm s^{-1}	500	Storm et al., 2020
Clupeidae	*Brevoortia tyrannus*	Atlantic menhaden	Ram	15 cm FL	Branchio-spinule	10 µm width	23 - 38 cm s^{-1}	2 - 3	Friedland, 1985
Clupeidae	*Clupea harengus*	Atlantic herring	Ram	25 cm SL	Denticle	98 µm width	34 cm s^{-1}, RF	14	Hamann et al., 2023
Clupeidae	*Dorosoma cepedianum*	Gizzard shad	Pump	29 cm SL	Gill raker	250 - 1500 µm width	35 - 70 cm s^{-1}	150 - 600	Sanderson et al., 2001
Clupeidae	*Sardina pilchardus*	Atlantic pilchard	Ram	12 cm SL	Denticle	91 µm width	41 cm s^{-1}, RF	16	Hamann et al., 2023
Clupeidae	*Sardinops sagax*	Pacific sardine	Ram	7.4 - 16.5 cm SL	Gill raker	23 - 38 µm width	7 - 24 cm s^{-1}	2 - 9	Rykaczewski, 2009
Cyprinidae	*Carassius auratus*	Goldfish	Pump	17 cm SL	Gill raker	250 - 1500 µm width	35 - 70 cm s^{-1}	150 - 600	Sanderson et al., 2001
Engraulidae	*Engraulis encrasicolus*	Atlantic anchovy	Ram	10 cm SL	Denticle	85 µm width	35 cm s^{-1}, RF	13	Hamann et al., 2023
Engraulidae	*Engraulis mordax*	Northern anchovy	Ram	7.3 - 15.0 cm SL	Gill raker	110 - 130 µm width	7 - 20 cm s^{-1}	9 - 25	Rykaczewski, 2009
Mobulidae	7 *Mobula* species	Manta and devil rays	Ram	~ 340 - 500 cm disc length	Filter lobe pore	0.36 - 3.34 mm^2 average pore area		10-350	Paig-Tran et al., 2013
Mobulidae	*Manta birostris*	Manta ray	Ram		Distance between lobes	1.7 mm	55 cm s^{-1}	1075	Divi et al., 2018
Mobulidae	*Mobula tarapacana*	Manta ray	Ram		Distance between lobes	3.63 mm	30 cm s^{-1}	1115	Divi et al., 2018
Rhinco-dontidae	*Rhincodon typus*	Whale shark	Pump and Ram	~ 600 cm TL	Reticulated mesh pore	1200 µm width		300	Motta et al., 2010
Scombridae	*Rastrelliger kanagurta*	Indian mackerel	Ram	21 cm SL	Denticle	593 µm width	47 cm s^{-1}, RF	121	Hamann et al., 2023
Scombridae	*Scomber scombrus*	Atlantic mackerel	Ram	27 cm SL	Denticle	592 µm width	50 cm s^{-1}, RF	128	Hamann et al., 2023

The column for filter element size lists the measurement of the dimension that was used for the Re calculation; flow speed is the speed used for the calculation at the level of the filter element. FL, fork length; RF, not including reduction factor of 42.3% used in Re calculation to account for hydrodynamic drag inside oral cavity; SL, standard length; TL, total length.

cavity via gaps between the GRs and associated protrusions, although the extent to which there are larger gaps between the tips of GRs on adjacent BAs or between the tips of GRs on the first BA and the internal walls of the oral cavity during SF is not known. For consistency among diverse SF animals and industrial filtration, the gaps will be referred to here as pores, with the important caveat that the gaps between the filter elements of SF fishes tend to have the three-dimensional shape of elongated slots with a height as well as a width and length (Sanderson et al., 2016; Storm et al., 2020). Multi-species analyses of the 2D and 3D shapes for pores between the filter elements of SF fishes have not been conducted (but see Hamann et al., 2023, for 2D mesh shapes and sizes).

The ecological and morphological diversity of SF fishes extends to the level of the smallest filter elements: the GRs and associated protrusions (Figure 3). Comprehensive ultrastructural comparisons of the locations and morphology of GRs and their protrusions in multiple taxa are rare for SF or non-SF fishes (but see extensive morphological and functional analyses of Hamann et al., 2023, and compilation of published studies in Storm et al., 2020). The degree of detail needed for physical and computational models necessitates the use of scanning electron microscopy, histology, confocal microscopy, and/or micro-CT scanning, ideally including quantitative data on size and shape changes resulting from preservation and preparation or from limitations in resolving soft tissues (e.g., in micro-CT). Such data are lacking for almost all SF fish species (but see Paig-Tran et al., 2013; Paig-Tran and Summers, 2014; Cohen and Hernandez, 2018).

TABLE 2 Pore sizes reported between filter elements in SF fishes.

Family	Species	Common Name	Pump or Ram	Body Size	Dimension Measured	Pore Size	Reference
Cichlidae	*Oreochromis niloticus*	Nile tilapia	Pump	14 - 23 cm	Mean distance between GRs on BAs 1-4	340 - 500 µm	Ibrahim et al., 2015
Clupeidae	*Alosa sapidissima*	American shad	Ram	38 - 41 cm SL	Mean distance between denticles for each of five BAs	200 - 340 µm	Storm et al., 2020
Clupeidae	*Brevoortia tyrannus*	Atlantic menhaden	Ram	3.4 - 32.6 cm FL	Mean distance between branchiospinules on BAs 1-4	12 - 37 µm	Friedland et al., 2006
Clupeidae	*Clupea harengus*	Atlantic herring	Ram	29 cm TL	Mean minimum distance between denticles on BA 1	323 µm	Collard et al., 2017
Clupeidae	*Clupea harengus*	Atlantic herring	Ram	2.5 - 30 cm TL	Mean distance between GRs on BA 1	90 - 470 µm	Gibson, 1988
Clupeidae	*Dorosoma cepedianum*	Gizzard shad	Pump	5 - 25 cm SL	Cumulative frequency distributions of distances between GRs on BAs 1-5	~ 30 - 110 µm	Mummert and Drenner, 1986
Clupeidae	*Sardina pilchardus*	Sardine	Ram	21 cm TL	Mean minimum distance between denticles on BA 1	214 µm	Collard et al., 2017
Clupeidae	*Sardinops sagax*	Pacific sardine	Ram	8 - 16 cm SL	Distance between GRs on BA 1	190 - 280 µm	Rykaczewski, 2009
Cyprinidae	*Abramis brama*	Common bream	Pump	25 - 33 cm SL	Distance between GR ridges on BAs 1-5	~ 1000 µm	Hoogenboezem et al., 1991
Engraulidae	*Engraulis encrasicolus*	European anchovy	Ram	15 cm TL	Mean minimum distance between denticles on BA 1	216 µm	Collard et al., 2017
Engraulidae	*Engraulis mordax*	Northern anchovy	Ram	8 - 14 cm SL	Distance between GRs on BA 1	270 - 470 µm	Rykaczewski, 2009
Mobulidae	7 *Mobula* species	Manta and devil rays	Ram	~ 340 - 500 cm DL	Filter lobe pores on BA 3	0.36 - 3.34 mm^2 average pore area	Paig-Tran et al., 2013
Mobulidae	*Manta birostris*	Manta ray	Ram		Filter lobe pores	340 µm	Divi et al., 2018
Mobulidae	*Mobula tarapacana*	Manta ray	Ram		Filter lobe pores	1100 µm	Divi et al., 2018
Poly-odontidae	*Polyodon spathula*	American paddlefish	Ram	27 - 85.5 cm EFL	Mean distance between GRs in middle of BA 1	~ 40 - 65 µm	Rosen and Hales, 1981
Rhinco-dontidae	*Rhincodon typus*	Whale shark	Pump/Ram	593 - 622 cm TL	Mean reticulated mesh size, all filtering pads	900 - 1400 µm	Motta et al., 2010

Although the gaps between the filter elements are referred to here as two-dimensional pores, such gaps in SF fishes tend to have the three-dimensional shape of slots with a height as well as a width and length. Filter element height has been reported rarely. BA, branchial arch; DL, disc length; EFL, eye-to-fork length; FL, fork length; GR, gill raker; SL, standard length; TL, total length.

1.3 Filter media and particle separation

There is an important functional distinction between (1) SF animals in which all fluid passes through the filter medium due to the enclosure of the filter either within the mouth (e.g., fish, baleen whales) or within another body cavity (e.g., ascidians, bivalves) versus (2) the many SF invertebrate taxa in which water is not constrained to pass through the filter medium, i.e., the water can travel around the margins of the filter (e.g., cnidarians, crinoids, bryozoans) (Sanderson and Wassersug, 1993; Hamann and Blanke, 2022).

In many SF invertebrate taxa that have an unenclosed filter, particle capture requires contact (i.e., encounter) with a filter element such as a sticky mucus-covered tentacle or appendage on which the particle is then retained (Rubenstein and Koehl, 1977; Shimeta and Jumars, 1991). In contrast, because the filter medium of fish is enclosed inside the mouth, particles may remain suspended while traveling to the posterior of the mouth with minimal or no contact on the filter (Sanderson et al., 2001; Cheer et al., 2012). Alternatively in SF fishes, particles may contact the filter repeatedly by rolling or bouncing posteriorly (Divi et al., 2018; Witkop et al., 2023). Thus, unlike the case in many SF invertebrates, particle separation in SF fishes may occur without particle contact and/or without particle capture on the filter elements.

Throughout the biological and industrial filtration literature, there are inconsistencies in the definitions and uses of the terms filtration versus particle separation. Here, the more inclusive term particle separation will be used to refer broadly to solid-liquid separation processes that result in the retention and concentration of particles but do not necessarily involve particle capture on a

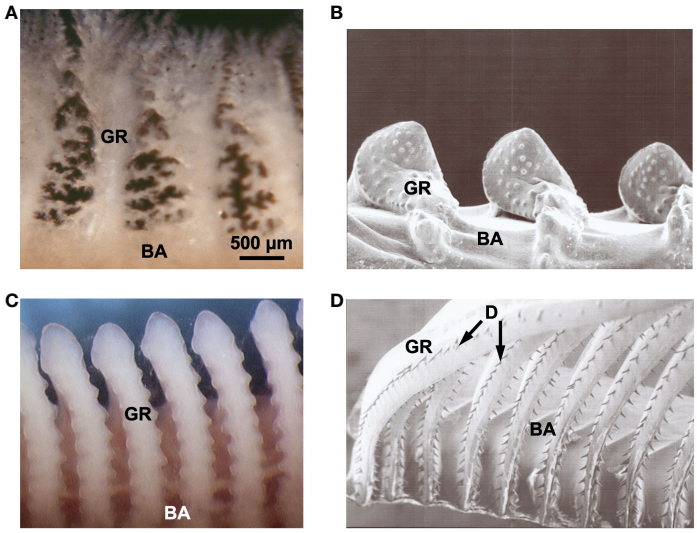

FIGURE 3
Examples of gill rakers in SF fish species belonging to three orders, shown in frontal view. **(A)** Pump SF Sacramento blackfish, *Orthodon microlepidotus*, Cyprinidae, Cypriniformes (fresh specimen). **(B)** Pump SF Singida tilapia (ngege), *Oreochromis esculentus*, Cichlidae, Cichliformes (scanning electron microscopy, SEM). **(C)** Pump SF goldfish, *Carassius auratus*, Cyprinidae, Cypriniformes (fresh specimen). **(D)** Ram SF American shad, *Alosa sapidissima*, Clupeidae, Clupeiformes (SEM). 500 µm scale bar refers to all images. BA, branchial arch; D, denticles; GR, gill raker.

porous filter. While industrial and biomedical particle separation mechanisms can involve the passage of water through a porous filter medium often referred to as a membrane (e.g., Chew et al., 2020), particle separation can alternatively involve the passage of water through microfluidic devices and other non-porous pipes or channels that have solid walls instead of a filter medium (e.g., Tang et al., 2022; Lee et al., 2023). As discussed in later sections for SF fishes, most but not all proposed particle separation mechanisms involve the simultaneous passage of water through the filter medium, with the branchial arches, gill rakers, and associated protrusions serving as the filter.

2 Pump versus ram suspension feeding and pulsatile or oscillatory flow

Sanderson and Wassersug (1993) identified four categories of vertebrate suspension feeders based on the methods used to transport water into the mouth. Here, SF fishes will be referred to as either pump suspension feeders ("intermittent suction feeders") or ram suspension feeders ("continuous ram feeders"), depending on the method of generating water flow through the oral and opercular cavities (Sanderson and Wassersug, 1993).

The functional morphology and hydrodynamics of pump SF appear similar to suction feeding in fish, but pump SF consists of a series of repetitive pumps. Pump suspension feeders either remain stationary or swim forward slowly while pumping. In contrast, ram (also referred to as "tow-net", Lazarro, 1987) suspension feeders swim forward with an open mouth to engulf water continuously as the filtrate exits from beneath the flared opercular bones. At intervals ranging from seconds to minutes, pump SF and ram SF are interrupted by prey processing movements that are thought to transport, aggregate, and/or enable swallowing of prey (e.g., Sanderson et al., 1991; Sanderson et al., 1996b; Hamann et al., 2023).

Experiments using high-speed endoscopic videos, thermistor flow probes, pressure transducers, and high-speed X-ray particle tracking have established that flow through fish oral cavities during SF is pulsatile and/or oscillatory (e.g., Sanderson et al., 1991, Sanderson et al., 1994; Callan and Sanderson, 2003; Haines and Sanderson, 2017; Provini et al., 2022). Pulsatile flow involves repetitive cycles of increasing and subsequently decreasing flow speed, whereas oscillatory flow is defined by periodic reversals in flow direction. In pump SF species, these dynamic flows are caused by changes in oral cavity volume as the BAs abduct and adduct in three dimensions, resulting in flow reversals (i.e., from posterior to anterior) that contribute to particle and mucus suspension and transport (Sanderson et al., 1996b; Smith and Sanderson, 2008; Provini et al., 2022). As ram SF species swim forward with an open mouth, locomotor kinematics, particularly yaw and heave, cause pulsatile fluctuations in intra-oral flow speeds and pressures that reduce clogging (Haines and Sanderson, 2017). CFD simulations of fish SF that incorporate the underlying kinematics are problematic and few physical models have explored dynamic flow (Haines and Sanderson, 2017; Schroeder et al., 2019). This is a promising area for further research, as pulsatile and oscillatory flow have been shown to delay clogging in microfluidics and crossflow membrane microfiltration (e.g., Wang et al., 2021; Dincau et al., 2022).

3 Fundamental differences between SF in fishes versus invertebrates

While there is a rich history of research on filtration mechanisms in SF invertebrates (reviews in Jørgensen, 1966; Riisgård and Larsen, 2010; Hamann and Blanke, 2022), relatively

few studies on the biomechanics and fluid dynamics of vertebrate SF have been conducted, with most published after Sanderson and Wassersug (1993). Relevant data and models for SF fishes are rare, particularly with respect to the 3D spatially and temporally variable size, shape, and fluid dynamics of the oral cavity (e.g., Divi et al., 2018; Paskin et al., 2022; Van Wassenbergh and Sanderson, 2023; Witkop et al., 2023).

Despite limitations in our knowledge, the novel particle separation mechanisms proposed recently for SF fishes (Sanderson et al., 2001; Cheer et al., 2012; Sanderson et al., 2016; Cohen et al., 2018; Divi et al., 2018; Witkop et al., 2023) appear to be fundamentally distinct from those described for invertebrates. Due to the morphological and ecological diversity of SF fishes and SF invertebrates, broad generalizations are difficult. However, based on SF fish research published during the past twenty years, a suite of differences between the structures and fluid dynamics of SF fishes versus most SF invertebrates is identified below in this section. Together, these differences indicate that the particle separation mechanisms of SF fishes can be anticipated to extend beyond the hydrodynamic principles applied for particle separation in SF invertebrates.

3.1 Fishes are active suspension feeders

Unlike many subphyla or phyla of SF invertebrates (Hentschel and Shimeta, 2019), all SF fishes are active rather than passive suspension feeders, i.e., actively generate a flow of water into and through their oral cavity. In addition, the filter elements of SF fishes are completely enclosed within a roughly conical oral cavity (Cheer et al., 2001; Sanderson et al., 2016; Brooks et al., 2018; Witkop et al., 2023), which serves as the equivalent of the channel or pipe in industrial filtration and microfluidics. Active SF using an enclosed filter medium results in the potential ability to (a) control and adjust pore sizes as well as flow speed and direction along and between the filter elements (e.g., Sanderson et al., 1991; Provini et al., 2022), (b) control the pressure differential across the filter (e.g., Haines and Sanderson, 2017; Divi et al., 2018), and (c) employ particle separation mechanisms that require flow in pipes and channels for optimal operation (e.g., Sanderson et al., 2001; Cheer et al., 2012; Sanderson et al., 2016; Divi et al., 2018; Witkop et al., 2023), as discussed further below.

3.2 Large filter element sizes and flow speeds in fishes

Advantages of active SF using an enclosed filter medium are detailed above in section 3.1. In addition, the sizes of the filter elements between which water passes, and the flow speeds at the filter, tend to be larger in SF fishes than in SF invertebrates. Consequently, Reynolds numbers calculated at the level of the proposed filter elements in SF fishes range from ~ 2 – 1115 across two orders of magnitude in body size (~10 cm – 6 m, Table 1).

3.3 Large pore sizes in fishes

The available data on SF fishes are not sufficient for statistical comparisons of pore sizes between filter elements in SF fishes versus SF invertebrates relative to particle sizes in the diet and body size of the suspension feeder. However, while some SF fish species have small pore sizes (e.g., as small as 12 μm in juvenile menhaden, Friedland et al., 2006), the pore sizes can be relatively large in SF fishes (frequently 100 – 500 μm, Table 2).

4 Distinct hydrodynamic configurations: dead-end versus crossflow

In SF fishes, two distinct hydrodynamic configurations for the orientation of the filter with respect to the approaching flow have been proposed: dead-end and crossflow. The hydrodynamic configuration that is used is of fundamental importance because the orientation of the filter determines the types of particle separation mechanisms that are feasible. Historically, these configurations have been referred to in the primary literature as “dead-end filtration” and “crossflow filtration”.

4.1 Dead-end configuration

Dead-end has been the conventional configuration hypothesized for SF fishes (Gerking, 1994; Ross, 2013). In dead-end filtration (Figure 4A), the fluid to be filtered travels approximately perpendicular (approximately orthogonal or “normal”, i.e., ~ 90 degrees) to the filter medium, such that there are two streams of fluid: (1) the mainstream flow (i.e., the freestream flow or feed flow of unfiltered fluid) that approaches the GRs and (2) the filtrate (i.e., permeate) that has passed between the GRs. Filtrate is forced between the GRs by higher pressures inside the oral cavity relative to the opercular cavities. In the dead-end configuration, particles are trapped on the GRs when the particles are too large to pass through the gaps (pores) (Rubenstein and Koehl, 1977; LaBarbera, 1984; Shimeta and Jumars, 1991). Therefore, hypotheses for particle separation mechanisms using dead-end filtration in SF fishes are limited to sieving of particles that are equal to or larger than the pore size and/or mucus entrapment of particles with sizes that can be less than the pore size.

4.2 Crossflow configuration

Dead-end filtration was the sole hydrodynamic configuration considered for porous filters in SF vertebrates until crossflow filtration was discovered in SF fishes (Figure 4B). When a miniature fiberoptic endoscope was inserted through a dermal bone into the oral cavities of unrestrained fish as they pump suspension fed freely (goldfish, *Carassius auratus*, Cyprinidae; ngege or Singida tilapia, *Oreochromis esculentus*, Cichlidae;

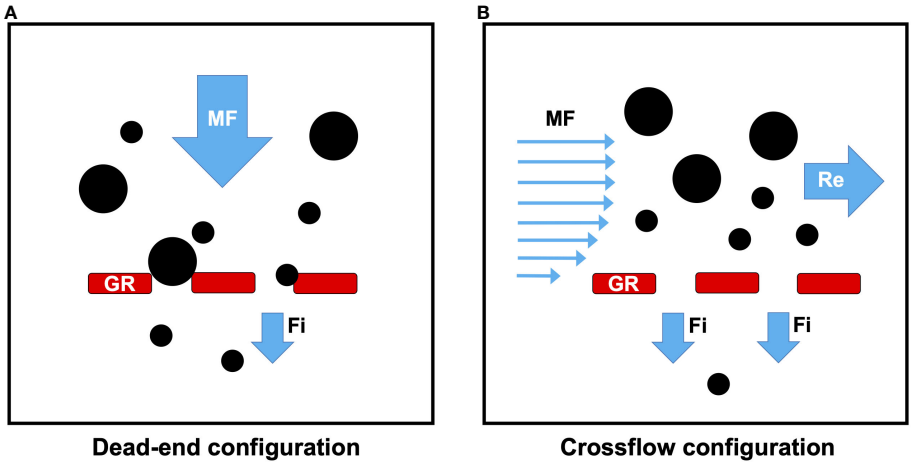

FIGURE 4
The two hydrodynamic configurations in SF fishes: dead-end versus crossflow. Gill rakers (red) are shown in cross-section. **(A)** In the dead-end configuration, the fluid to be filtered (mainstream flow) approaches the GRs at an angle of approximately 90 degrees while the filtrate passes through the gaps between the GRs (i.e., through the GR pores). Particles (black) that are larger than the GR pores are captured by direct sieving on the GR surfaces. In the dead-end configuration, particles that are smaller than the GR pores are captured only if particle flocculation or clumping occurs on the GR surface or inside the GR pores, or if mucus entrapment occurs on an adhesive GR surface. **(B)** In the crossflow configuration, the flow approaching the GRs travels tangentially or approximately parallel to the GRs before exiting as filtrate. However, particles are carried posteriorly in crossflow along the GRs of SF fishes, resulting in the formation of a retentate or concentrate of particles (Brainerd, 2001; Sanderson et al., 2001). Due to the tangential flow across the GRs in the crossflow configuration, particles can be retained inside the oral cavity using particle separation mechanisms other than or in addition to sieving and mucus entrapment, including inertial lift and shear-induced migration, reduction of effective gap size by vortices, vortical flow along outer faces of gill raker plates, cross-step filtration, ricochet filtration, and lateral displacement. Fi, filtrate; GR, gill rakers; MF, mainstream flow; Re, retentate.

gizzard shad, *Dorosoma cepedianum*, Clupeidae), dead-end filtration did not occur on GR surfaces and particles were not trapped in mucus (Sanderson et al., 2001). Instead, particles (40 μm – 1 mm diameter) were transported in flow moving along the channel between the roof and the floor of the oral cavity, traveling approximately parallel to the GRs. Particles that contacted the GRs infrequently did not accumulate on GR surfaces and were instead carried posteriorly in the oral cavity toward the esophagus. Sanderson et al. (2001) identified this unexpected hydrodynamic configuration as crossflow filtration. The crossflow configuration has also been proposed for balaenopterid (Goldbogen et al., 2007; Potvin et al., 2009) and balaenid whales (Werth and Potvin, 2016).

Since the 1980s, crossflow has been the preferred configuration for the industrial microfiltration of beverages and foods (e.g., fruit juices, beer, dairy products), although the dead-end configuration continues to be used as an option for dilute feeds (e.g., drinking water treatment) (Chew et al., 2020). More recently, the crossflow configuration reported in SF fishes has inspired crossflow systems for oil-water separation (Dou et al., 2017; Li et al., 2018) that have then stimulated extensive further research on similar uses of the crossflow configuration with superwetting membranes. Prior to the bioinspired crossflow configuration, membranes for oil-water separation had been used in a gravity-driven dead-end configuration that led to rapid fouling of the membranes by oil (Su et al., 2021).

Crossflow filtration is also known as tangential filtration because the flow approaching the GRs travels tangentially or approximately parallel to the GRs, i.e., along and over the GRs inside the oral cavity. Hamann et al. (2023) proposed the term "semi-cross-flow filtration" to differentiate crossflow configurations in which the tangential flow is between 0 and 90 degrees. During crossflow filtration, higher pressure inside the oral cavity of SF fishes (relative to the pressure of the fluid that is located immediately external of the GRs) causes filtrate to exit between the GRs. However, particles can be carried posteriorly in crossflow along the GRs of SF fishes, resulting in the formation of a retentate or concentrate of particles suspended in a limited volume of water near the terminus of the oral cavity (Brainerd, 2001; Sanderson et al., 2001). Due to the tangential flow across the GRs during crossflow filtration, particles can be retained inside the oral cavity using particle separation mechanisms other than or in addition to sieving and mucus entrapment.

4.3 Major advantages of the crossflow configuration

In SF fishes, there are three major advantages of the crossflow configuration compared to the dead-end configuration. The net outcome of these advantages is that the crossflow configuration could result in the retention of particles that are smaller than the distances between filter elements, while transporting particles toward the esophagus without accumulation of particles on the filter surfaces and therefore with reduced clogging.

4.3.1 Transport concentrated particles, reducing clogging

Dead-end filters are designed to retain particles by clogging, but this clogging causes the filter to cease functioning and therefore requires a separate process for the removal of particles from the filter. In SF fishes using the crossflow configuration, as the filtrate

exits through the pores between GRs, the tangential shear force of the crossflow along the filter surfaces minimizes the accumulation of particles on the filter. The crossflow transports concentrated particles downstream, thereby reducing clogging (Sanderson et al., 2001). During *in vivo* endoscopic observations of crossflow filtration in pump SF fishes, the crossflow that travels across the GR surfaces (as fast as ~ 55 cm s^{-1}, Sanderson et al., 1991) has been observed to transport suspended particles, or particles aggregated in mucus strands, posteriorly toward the esophagus (Sanderson et al., 1991; Sanderson et al., 1996b, Sanderson et al., 2001).

4.3.2 Retain particles smaller than pore sizes

Particles that are smaller than the pore sizes between filter elements cannot be retained using a non-adhesive filter in the dead-end configuration, unless such smaller particles flocculate (i.e., clump) or are retained in pores that are already partially clogged as suggested by Friedland et al. (1984). In the crossflow configuration, a number of particle separation mechanisms have been proposed that could retain particles smaller than the pore sizes (e.g., Sanderson et al., 2001; Cheer et al., 2012; Sanderson et al., 2016; Divi et al., 2018; Witkop et al., 2023). Therefore, pore sizes could evolve to target the retention of small particles with minimal clogging in the crossflow configuration.

4.3.3 Generate vortical flow

As the approaching flow passes tangentially along the filter elements inside the oral cavity during crossflow filtration, vortical flow is generated inside the gaps between BAs and/or between GRs (Cheer et al., 2012; Sanderson et al., 2016). Dead-end filtration has not been proposed to result in vortical flow that could play a role in the filtration process. In contrast, the vortical flow that results from crossflow is an important component of all recently hypothesized particle separation mechanisms in fish (Cheer et al., 2012; Sanderson et al., 2016; Cohen et al., 2018; Divi et al., 2018; Witkop et al., 2023).

5 Proposed particle separation mechanisms in SF fishes

Suspension-feeding processes are extremely difficult to observe or quantify inside the oral cavity of live fish. Therefore, SF mechanisms have often been inferred from gut contents, X-ray or endoscopic videos of particle retention in live fish, physical modeling, and computational fluid dynamics (CFD) simulations. Although multiple hypotheses have been proposed for particle separation mechanisms at the level of the GRs and associated protrusions, limited published evidence supports each mechanism in specific species (Table 3) and no clear consensus has emerged on broader patterns or unifying principles based on morphology, function, or taxonomy. Synthesis of the data available thus far indicates that particle separation mechanisms can differ between SF fish species belonging to the same family or genus (e.g., Goodrich et al., 2000), and may differ even within species depending on the type or size of particle being retained (e.g., Sanderson et al., 1996b; Callan and Sanderson, 2003). Here, each of the proposed particle separation mechanisms is discussed with a focus on unresolved questions and current challenges.

5.1 Sieving

Shimeta and Jumars (1991) noted that sieving is best considered as a particle retention mechanism, not a particle encounter mechanism. During sieving, also referred to as mechanical sieving or direct sieving in suspension feeders (Riisgård and Larsen, 2010; Conley et al., 2018a), particles are retained on the filter elements when the particle size is larger than the pore size (Rubenstein and Koehl, 1977; LaBarbera, 1984; Shimeta and Jumars, 1991).

In theory, if all gaps between GRs have the same minimum dimension, sieving in SF fishes could be identified by a distinct threshold in the minimum size of the retained particles, i.e., the retained particles would include 100% of the particles larger than the gap size but none smaller. In practice, the sizes of the gaps between GRs of SF fishes can vary within and among BAs as well as vary when the mouth is opened and closed during a pumping cycle or during ram SF (e.g., Mummert and Drenner, 1986; Gibson, 1988). In addition, the entrapment of small particles in mucus on the GRs during sieving could result in the capture of particles that are smaller than the gap size.

Historically, mechanical sieving in the dead-end configuration has been the conventional view of fish SF (LaBarbera, 1984; Gerking, 1994; Ross, 2013, Figures 5A, B). From primary literature (1984-1994), Sanderson et al. (1996b) summarized six proposed locations for sieving between different filter elements (e.g., between lateral and medial GRs on adjacent BAs, between adjacent GRs on a single BA, between denticles, etc.). Based on congruence between pore sizes and the particle sizes in gut contents, sieving has been proposed recently as the primary or sole particle separation mechanism in several SF fish species belonging to the families Clupeidae and Engraulidae (e.g., Friedland et al., 2006; Rykaczewski, 2009; Idris et al., 2016; Collard et al., 2017). For example, Mummert and Drenner (1986) quantified the sizes and numbers of microspheres (10 – 80 μm diameter) and zooplankton in water samples taken while gizzard shad fed in laboratory experiments. They reported that the particle-size-dependent removal of microspheres and zooplankton in water samples was consistent with their model of filtering efficiency based on the cumulative frequency of inter-raker distances measured in preserved gizzard shad.

However, the retention of prey that are smaller than the pore sizes has been reported for certain prey types and fish size classes in some of the species for which sieving has been proposed, leading the authors to suggest that other particle separation mechanisms may be operating in addition to or instead of sieving (Friedland et al., 2006; Rykaczewski, 2009). Mechanical sieving has not been observed endoscopically in the three tilapia species, two cyprinid species, and one clupeid species that have been studied during pump SF (Sanderson et al., 1991; Sanderson et al., 1996b; Goodrich et al., 2000; Sanderson et al., 2001; Callan and Sanderson, 2003; Smith and Sanderson, 2008). Particle retention has not been studied endoscopically *in vivo* for ram SF species.

TABLE 3 Particle separation mechanisms proposed in the primary literature for specific SF fish species.

Family	Species	Common Name	Pump or Ram	Proposed Particle Separation Mechanism	Reference
CICHLIDAE	*Oreochromis aureus*	Blue tilapia	Pump	Inertial lift/Shear-induced migration	Smith and Sanderson, 2007, 2013
	Oreochromis esculentus	Ngege (Singida) tilapia	Pump	Inertial lift/Shear-induced migration	Sanderson et al., 2001; Smith and Sanderson, 2013
	Oreochromis niloticus	Nile tilapia	Pump	Mucus entrapment	Northcott and Beveridge, 1988; Sanderson et al., 1996b
CLUPEIDAE	*Alosa sapidissima*	American shad	Ram	Cross-step filtration (with dead-end filtration near esophagus)	Storm et al., 2020
				Lateral displacement	Witkop et al., 2023
	Brevoortia tyrannus	Atlantic menhaden	Ram	Sieving	Friedland, 1985; Friedland et al., 2006
	Clupea harengus	Atlantic herring	Ram	Sieving	Gibson, 1988; Collard et al., 2017
				Crossflow filtration (with dead-end filtration near esophagus)	Hamann et al., 2023
	Dorosoma cepedianum	Gizzard shad	Pump	Sieving	Drenner et al., 1984; Mummert and Drenner, 1986
				Inertial lift/Shear-induced migration	Sanderson et al., 2001
	Sardina pilchardus	Sardine	Ram	Sieving	Collard et al., 2017
				Crossflow filtration (with dead-end filtration near esophagus)	Hamann et al., 2023
	Sardinops sagax	Pacific sardine; southern African sardine	Ram	Sieving	Rykaczewski, 2009; Idris et al., 2016
CYPRINIDAE	*Abramis brama*	Common bream	Pump	Sieving	van den Berg et al., 1993; van den Berg et al., 1994b
	Blicca bjoerkna	White bream	Pump	Sieving	van den Berg et al., 1993; van den Berg et al., 1994b
	Carassius auratus	Goldfish	Pump	Inertial lift/Shear-induced migration	Sanderson et al., 2001
	Cyprinus carpio	Carp	Pump	Sieving	van den Berg et al., 1994b
				Crossflow filtration	Callan and Sanderson, 2003
	Hypophthalmichthys molitrix	Silver carp	Pump	Vortical flow along outer faces of gill raker plates	Cohen and Hernandez, 2018
	Hypophthalmichthys nobilis	Bighead carp	Pump	Crossflow filtration	Cohen and Hernandez, 2018
	Orthodon microlepidotus	Sacramento blackfish	Pump	Mucus entrapment	Sanderson et al., 1991
	Rutilus rutilus	Roach	Pump	Sieving	van den Berg et al., 1993; van den Berg et al., 1994b
ENGRAULIDAE	*Engraulis anchoita*	Argentine anchovy	Ram	Sieving	Ciechomski, 1967
	Engraulis encrasicolus	European anchovy	Ram	Sieving	Collard et al., 2017
				Crossflow filtration (with dead-end filtration near esophagus)	Hamann et al., 2023
	Engraulis mordax	Northern anchovy	Ram	Sieving	Rykaczewski, 2009
MUGILIDAE	> 10 mugilid genera	Mullet	Pump	Sieving	Harrison and Howes, 1991
MOBULIDAE	~ 9 *Mobula* species	Manta and devil rays	Ram	Sieving	Paig-Tran et al., 2013
	Manta birostris	Manta ray	Ram	Ricochet filtration	Divi et al., 2018
	Mobula tarapacana	Manta ray	Ram	Ricochet filtration	Divi et al., 2018

(Continued)

TABLE 3 Continued

Family	Species	Common Name	Pump or Ram	Proposed Particle Separation Mechanism	Reference
RHINCO-DONTIDAE	*Rhincodon typus*	Whale shark	Pump/Ram	Crossflow filtration	Motta et al., 2010
SCOMBRIDAE	*Rastrelliger kanagurta*	Indian mackerel	Ram	Crossflow filtration (with dead-end filtration near esophagus)	Hamann et al., 2023
	Scomber scombrus	Atlantic mackerel	Ram	Crossflow filtration (with dead-end filtration near esophagus)	Hamann et al., 2023

Two rows are provided for species in which two separation mechanisms have been proposed. Crossflow filtration is listed for species that were reported to use the crossflow configuration but for which a more specific particle separation mechanism was not reported.

5.2 Mucus entrapment and particle transport

During hydrosol filtration, a number of fluid mechanical processes (e.g., direct interception and inertial impaction) can cause particles to encounter a filter surface that has adhesive properties (Rubenstein and Koehl, 1977; Shimeta and Jumars, 1991). Particles can then be retained by adhesion to the mucus-covered surface of the filter. Note that the particle encounter mechanisms (e.g., direct interception, inertial impaction) occur independently of the particle capture mechanism (e.g., the sticky filter surface) (Shimeta and Jumars, 1991). This section focuses on particle separation that results from adhesion of particles to mucus-covered filter surfaces, including the roles of mucus in particle aggregation and transport.

Mucus is a viscoelastic heterogeneous hydrogel with adhesive properties, consisting primarily of glycosylated proteins termed

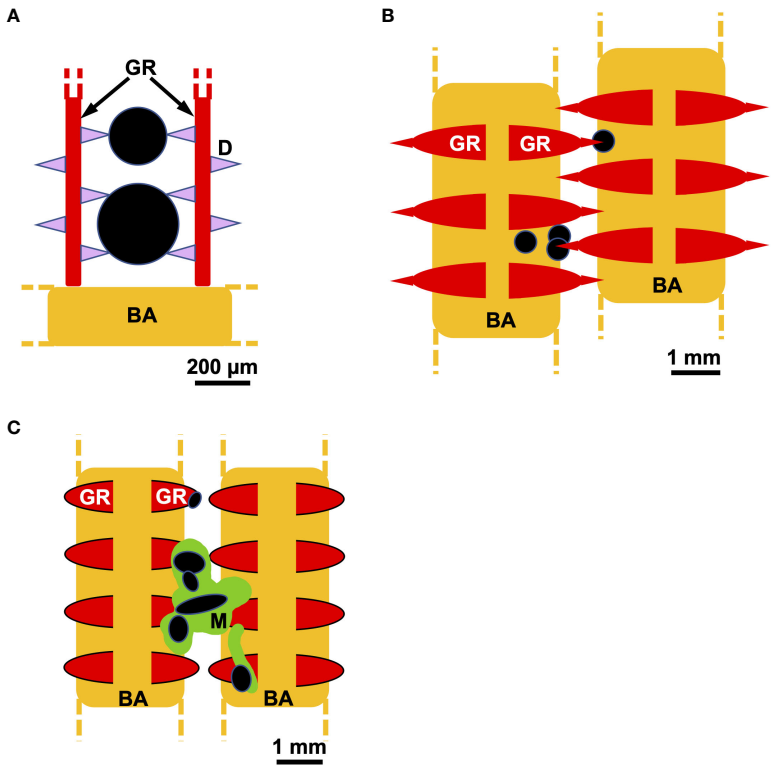

FIGURE 5
Schematic examples of direct sieving versus mucus entrapment, shown in frontal view. **(A)** Denticles (pink), gill rakers (red), and branchial arches (gold) have been proposed to connect to form a sieve that captures particles (black) in ram SF species such as herring (Clupeidae) and anchovy (Engraulidae) (e.g., Gibson, 1988; Collard et al., 2017). **(B)** Gill rakers, including protrusions that may be movable, have been proposed to form a branchial sieve that can capture particles in the channels between the gill rakers in pump SF species such as common bream and carp (Cyprinidae) (e.g., Hoogenboezem et al., 1991; van den Berg et al., 1994a, van den Berg et al., 1994b). **(C)** In pump SF Nile tilapia (Cichlidae), strands or aggregates of mucus (green) on the gill rakers and branchial arches have been observed in endoscopic videotapes to capture particles that were otherwise small enough to pass between the filter elements. Subsequently, particle-laden mucus was observed to be transported posteriorly in crossflow toward the esophagus (Sanderson et al., 1996b). Dashed lines indicate that structures repeat. BA, branchial arch; D, denticle; GR, gill raker; M, mucus.

mucins (Cerullo et al., 2020; Bayer, 2022). Mucins and mucin-like proteins are found in taxa throughout the Metazoa (Lang et al., 2016), and the use of mucus for SF is widespread among invertebrates (Hamann and Blanke, 2022). Multiple types of mucin proteins are ubiquitous in vertebrate taxa and are essential for many respiratory, digestive, reproductive, and immunological functions (Shephard, 1994; Lang et al., 2016; Bansil and Turner, 2018).

Mucus-secreting cells (e.g., goblet cells) are typically found in fish oral epithelia, on or near the GRs as well as on the gill filaments. Based on the locations of mucus-secreting cells identified in the oral cavity, the use of mucus for particle separation and/or transport has been proposed in multiple taxa of SF fishes (e.g., Atlantic menhaden, *Brevoortia tyrannus*, Clupeidae, Friedland, 1985; three species of rays, *Mobula*, Mobulidae, Paig-Tran and Summers, 2014; silver carp and bighead carp, *Hypophthalmichthys molitrix* and *Hypophthalmichthys nobilis*, Cyprinidae, Cohen and Hernandez, 2018; American shad, *Alosa sapidissima*, Clupeidae, Storm et al., 2020; earlier studies summarized in Sanderson et al., 1996b). In endoscopic videotapes, omnivorous pump SF Nile tilapia (*Oreochromis niloticus*, Cichlidae) were observed to retain particles (40 μm – 1 mm diameter) in mucus strands or aggregates on the GR surfaces (Sanderson et al., 1996b, Figure 5C). However, despite belonging to the same genus and specializing on phytoplankton and colonial blue-green algae, the ngege tilapia *O. esculentus* was not observed endoscopically to have mucus strands or aggregates on or near the GRs during pump SF, and particles were not retained on any oral surfaces (Goodrich et al., 2000).

The physical properties of mucus, such as viscosity and electrostatic charge, can vary with the type of cell that secretes the mucus and therefore can vary with location inside the oral cavity (Friedland, 1985; Sibbing and Uribe, 1985; Northcott and Beveridge, 1988). While mucus properties are of substantial biomedical interest, there are few studies on the biochemistry and biomechanics of mucus in fish oral cavities. Bulusu et al. (2020) have provided the first macro-rheological study of oral mucus for a fish species, including shear thinning. Such data for SF fishes are important because shear thinning of mucus within a boundary layer or a vortical flow has the potential to enable particle transport processes that could be essential components of particle separation mechanisms.

Available data are not sufficient to assess whether there are interspecific or intraspecific patterns in mucus occurrence and mucus-secreting cell locations and abundance based on food particle type, pump versus ram SF, fish body size, or particle separation mechanism. A useful first step for further study could be to identify specific SF fish species that lack mucus-secreting cells on filter element surfaces. For example, Friedland (1985) noted that mucus cells are absent on Atlantic menhaden branchiospinules, small protrusions on the GRs. Therefore, he concluded that menhaden use mechanical sieving to retain particles on the branchiospinules. Another productive future approach could be to incorporate synthetic hydrogels and other mucus analogues (e.g., Authimoolam and Dziubla, 2016; Bej and Haag, 2022) into computational models as done with drag-reducing agents and microgrooves (Zhang et al., 2022a), or into physical models as suggested by Witkop et al. (2023).

As is the case for sieving, mucus entrapment of particles is potentially problematic because the trapped particles must be transported posteriorly toward the esophagus for swallowing. However, mucus can serve as both a particle aggregation and particle transport medium. The hydrodynamics of particle transport in the oral cavity of SF and non-SF fishes are one of the least understood aspects of fish feeding (Sanderson and Wassersug, 1993; Cheer et al., 2001; Day et al., 2015; Provini et al., 2022). Limited data are available on particle transport processes in SF fishes. When SF Nile tilapia interrupted a series of pumps periodically to perform a prey-handling process termed a post-pump flow reversal, particle-laden mucus was observed endoscopically to lift slightly from the GRs and travel briefly in an anterior direction in association with hyoid and branchial arch abduction during closed premaxillary protrusion (Sanderson et al., 1996b). The subsequent resumption of pump SF transported the mucus posteriorly toward the esophagus. Hoogenboezem and van den Boogaart (1993) described boluses of mucus containing large numbers of zooplankters (up to 900 in a single bolus) inside the oral cavities of freshly caught common bream (*Abramis brama*, Cyprinidae). van den Berg et al. (1994a) suggested that the zooplankters were trapped in the bream's branchial sieve initially (Figure 5B) but were then coated by mucus and aggregated during flow reversals termed back-washing.

Another process by which mucus may serve to aggregate and transport particles involves the epibranchial organs. Epibranchial organs are bilaterally paired muscular sac-like structures in the posterior oral cavity near the esophagus that aggregate small prey in at least five SF and detritivorous otomorphan fish families (e.g., many clupeid and engraulid species and two cyprinid species, Cohen et al., 2022). Epibranchial organs have abundant mucus-secreting cells and chemosensory cells and appear to receive minute prey that have been transported along the rows of GRs that extend into the organs. Subsequently, the epibranchial organs are thought to expel boli of food-laden mucus into the posterior pharynx for swallowing (Hansen et al., 2014; Cohen et al., 2020). Detailed studies on morphology, development, and evolution have only recently been conducted for a subset of the more than seven types of epibranchial organs that have been described (Cohen et al., 2022). Given that particle aggregation and transport are integral components of fish SF, the roles of mucus and the epibranchial organs in these processes deserve further study.

Holley et al. (2015) developed an experimental protocol and equations for calculating mucus content in the epibranchial organs and the foregut of pump SF gizzard shad. They reported that mucus constituted an average of 12% of the epibranchial organ content and 10% of the foregut content by dry mass, indicating the importance of mucus for pump SF in gizzard shad. However, mucus entrapment of particles (40 μm – 1 mm diameter) was not observed endoscopically on the GRs of gizzard shad, and particles rarely contacted the filter elements during SF (Sanderson et al., 2001). Thus, the available data suggest that mucus may be used for particle transport in gizzard shad rather than as a particle separation mechanism.

5.3 Inertial lift and shear-induced migration

In industrial filtration using the dead-end configuration, sieving separates particles by retaining them on the filter medium. In contrast, in inertial microfluidics and industrial membrane microfiltration using the crossflow configuration, inertial lift and shear-induced migration aid in particle separation by causing particle migration across streamlines and away from the porous or non-porous walls of the channel or pipe, thereby reducing particle contact with the walls. Inertial lift and shear-induced migration cause larger particles to migrate farther than smaller particles from the walls of an inertial microfluidics channel or from a microfiltration membrane with small pore sizes (Belfort et al., 1994; Di Carlo et al., 2007). Therefore, in inertial microfluidics devices, particles can be separated by size within the main channel at equilibrium positions that are specific distances from the walls (Di Carlo, 2009; Di Carlo et al., 2009). Such size-segregated particles can then be collected from the main channel using outlets in specific locations.

Inertial lift has been observed in experiments with particles as large as ~ 1 mm in diameter (Martel and Toner, 2014), and shear-induced migration has been quantified for particles with diameters up to 30 μm (Schroën et al., 2017). The crossflow configuration takes advantage of inertial lift forces and shear-induced migration for the separation of particles smaller than approximately 10 – 20 μm diameter, including microalgae, bacteria, and blood cells (Di Carlo et al., 2007; Bouhid de Aguiar and Schroën, 2020; Xiang and Ni, 2022). In SF fishes that use the crossflow configuration, Sanderson et al. (2001) proposed that, rather than being a mechanical threshold for retention, particle size could be a hydrodynamic threshold that affects the magnitude of the lift and shear acting on particles at the interface between the crossflow and the filtrate flow.

Inertial lift (Figure 6) has also been referred to as inertial migration, inertial focusing, hydrodynamic lift, or the tubular pinch effect, but should not be confused with inertial impaction. Inertial lift is primarily the net result of two opposing forces known as the wall-induced lift ("wall effect") versus the shear-gradient induced lift (or shear-induced lift). Due to asymmetries in the flow profile around a particle near a wall and the net result of the wall-induced lift (directing the particle toward the channel center and away from the walls) versus the shear-gradient induced lift (directing the particle toward the walls and away from the channel center), inertial lift leads to differential particle migration across streamlines on the basis of particle size, generally at Re 1 – 100 (van Dinther et al., 2013b; Martel and Toner, 2014; Kumar and Das, 2022).

Shear-induced migration (Figure 7), most commonly modeled in membrane microfiltration, is also referred to as shear-induced diffusion or hydrodynamic diffusion, but should not be confused with hydrodynamic shear, tangential shear, or shear-gradient induced lift. Shear-induced migration causes particles to deviate from streamlines and move away from walls due to particle-particle interactions (Drijer and Schroën, 2018). These particle-particle interactions are affected by gradients in particle concentration, shear, and viscosity (Schroën et al., 2017; Di Vaira et al., 2022), particularly at high particle concentrations (van Dinther et al., 2013a; Dijkshoorn et al., 2017).

Although inertial lift and shear-induced migration are central to the fields of inertial microfluidics and crossflow membrane microfiltration, studies have not been conducted on the potential

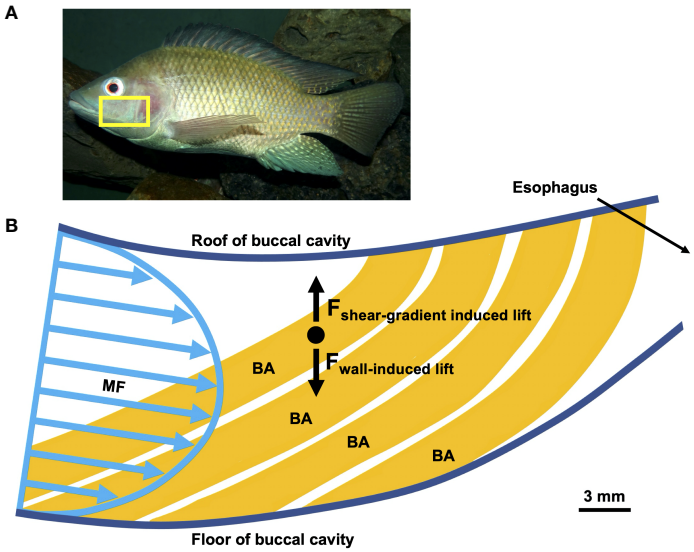

FIGURE 6
Schematic example of proposed inertial lift during crossflow in a generalized pump SF fish that is not using mucus entrapment (e.g., Sanderson et al., 2001; Smith and Sanderson, 2007, 2013). **(A)** The yellow box indicates the region of the oral cavity illustrated in **(B)**. Modified from © Bjørn Christian Tørrissen Bjørn Christian, CC BY-SA 3.0 https://creativecommons.org/licenses/by-sa/3.0/deed.en **(B)** Sagittal section through oral cavity, branchial arches in gold, spherical particle in black. During inertial lift in a pipe or channel, the wall-induced lift force acts opposite to the shear-gradient induced lift force. The net result is that particles migrate across streamlines to equilibrium positions in the pipe or channel (e.g., Di Carlo et al., 2009; Martel and Toner, 2014). These principles have been proposed to apply to SF fishes, including pump SF tilapia (Cichlidae) (e.g., Sanderson et al., 2001; Smith and Sanderson, 2007, 2013). Sagittal section in **(B)** modified from Sanderson et al. (2001), with permission. F, force; BA, branchial arch; MF, mainstream flow.

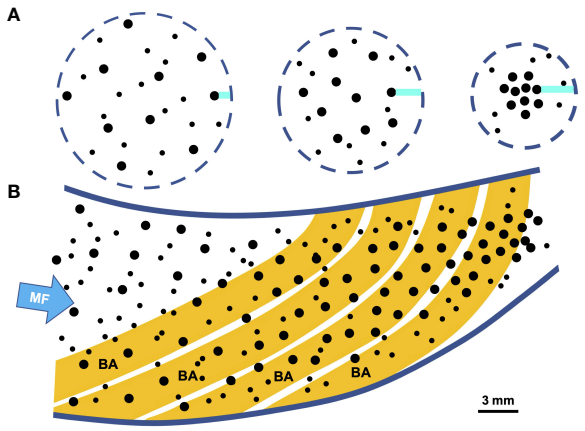

FIGURE 7
Schematic example of proposed shear-induced migration during crossflow in a generalized pump SF fish that is not using mucus entrapment (e.g., Sanderson et al., 2001). During shear-induced migration, particles deviate from streamlines and migrate away from walls due to particle-particle interactions, particularly at higher particle concentrations (e.g., van Dinther et al., 2013a; Drijer and Schroën, 2018). Larger particles migrate faster than smaller particles, resulting in separation of particles by size as smaller particles are lost through the pores in a porous tube or channel. **(A)** Frontal views (head-on) illustrating a suspension of small and large particles (black circles) in three cross-sections of a SF fish oral cavity shown sequentially from anterior (left) to posterior (right). Larger particles are proposed to migrate away from oral cavity surfaces more rapidly than smaller particles (indicated by the horizontal blue bars denoting increasing distance between larger particles and oral cavity surfaces as the oral cavity tapers posteriorly), while smaller particles are lost through the pores. **(B)** Sagittal section through oral cavity (branchial arches in gold), showing proposed concentration of predominantly larger particles away from walls as flow travels posteriorly. Cross-sections shown in **(A)** correspond approximately to locations from anterior to posterior along sagittal section in **(B)**. Panel **(B)** modified from Sanderson et al. (2001), with permission. BA, branchial arch; MF, mainstream flow.

importance of these hydrodynamic processes during crossflow at the scale of the pore sizes, Reynolds numbers, and channel diameters in SF fishes. For pump SF fishes, approximations have indicated that inertial lift would be at least an order of magnitude too low to account for the lack of particle contact with the GRs (Sanderson et al., 2001). However, those approximations were based on estimations of the channel Re, wall shear rate, and trans-raker pressure for the entire oral cavity of generalized suction-feeding fish, and did not account for GR shape or protrusions, oral cavity shape, or spatial/temporal variability during SF.

Clark and San-Miguel (2021) designed microfluidic devices (channel width 200 µm, channel height 60 µm) that scaled down the filter lobes and the target particle sizes used in research on ram SF manta rays (*Mobula birostris*, *M. tarapacana*; Divi et al., 2018) by approximately six times. Operating at Re ~ 1000 and a pore size of ~ 50 µm, these devices separated and concentrated particles (15 µm and 25 µm diameter) at a wide range of initial particle concentrations. The highest filtration efficiencies of 99% were achieved at inlet flow rates of 20 mL min^{-1}. Clark and San-Miguel (2021) referred to this as microfluidic "lobe filtration" and suggested that inertial lift forces play a key role. They demonstrated that the shapes of the scaled-down lobes caused complex velocity profiles in the device's main channel, and that calculations of the inertial lift forces resulting from the velocity profiles could predict the filtration efficiencies for particles of different sizes as the flow rate through the device was varied.

Since inertial lift and shear-induced migration require crossflow in an enclosed channel or pipe, and such prerequisites are found in relatively few invertebrate taxa (Hamann and Blanke, 2022), these processes have not yet been investigated in invertebrate SF. However, these processes may be relevant in some invertebrates, such as members of the subphylum Tunicata (e.g. appendicularians, thaliaceans, or ascidians, Morris and Deibel, 1993; Conley et al., 2018a, Conley et al., 2018b).

5.4 Reduction of effective gap size by vortices

Using CFD simulations of the complex posterior oral cavity in a generalized SF fish during crossflow filtration, Cheer et al. (2006, 2012) discovered and quantified a vortex located in each gap between the elliptical GRs (Figure 8). Subsequently, these were identified as trapped vortices that are generated because the GRs form a series of backward-facing steps in crossflow (Sanderson et al., 2016; also referred to as captive vortices, Divi et al., 2018). While these vortices appear similar to the trapped vortices used as flow control in aerodynamics and hydrodynamics (e.g., Lysenko et al., 2023), the proposed functions of the vortices for particle separation in SF fishes are unique because the trapped vortices are located in the slots (i.e., elongated gaps) between GRs rather than being located inside grooves with a solid floor (Sanderson et al., 2016).

Cheer et al. (2006, 2012) reported that the recirculating flow in the vortices partially blocked the flow of water between the GRs by preventing flow from exiting directly downstream of each GR. Therefore, each vortex served as a barrier that reduced the effective gap size by approximately 50% and led to particle retention in the mainstream flow. In CFD simulations, the vortices limited the exit of particles (82.5 – 160 µm diameter) through the gaps (250 µm) between the GRs, even though the particles were smaller than the gaps. The Reynolds numbers were 37.5 – 225, calculated using the major axis of the elliptical GRs and the mainstream flow speeds ranging from 10 – 60 cm s^{-1}. The specific flow patterns between the GRs varied depending on the speed and angle of the crossflow (60 – 75 degrees from the normal direction, i.e., the perpendicular, through the gap). Based on data from the simulations, Cheer et al. (2012) suggested that particle size and, to a lesser extent, particle density affected the inertial force and therefore affected the drag on particles as the particles deviated from the streamlines of water exiting between the GRs. The result was that particles were retained in the mainstream flow that continued toward the posterior of the oral cavity (Cheer et al., 2012).

Hung et al. (2012) and Hung and Piedrahita (2014) designed and tested a particle separator stated to be inspired by the computational models of Cheer et al. (2001, 2006, 2012). However, the structures of Hung et al. (2012) and Hung and Piedrahita (2014) differed substantially from SF fishes in shape,

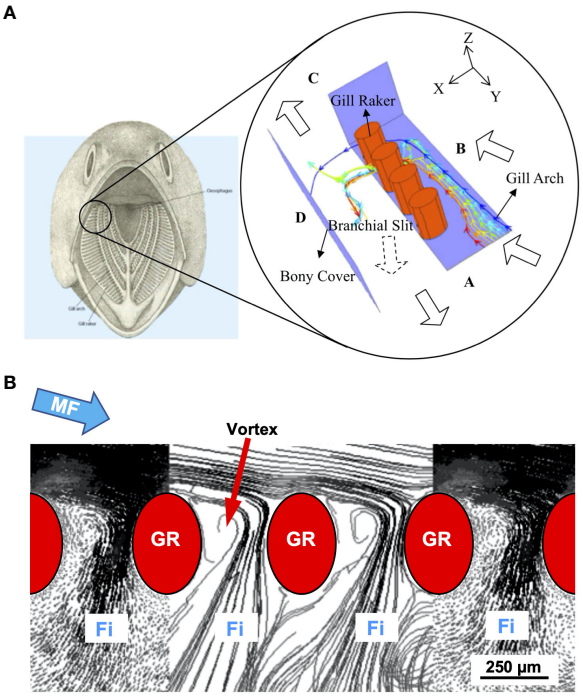

FIGURE 8
In CFD simulations of generalized SF fish, a vortex that formed in each gap between the elliptical gill rakers reduced the effective gap size by approximately 50% and led to particle retention in the mainstream flow (Cheer et al., 2006, 2012). **(A)** Geometric structure of the simulated oral cavity, showing placement of elliptical gill rakers (red). **(B)** Series of GRs with velocity vectors and path lines for flow along and between the GRs, including vortex that was generated posterior of each GR in crossflow at a mainstream flow speed of 60 cm s^{-1}, Re = 225. Adapted from Cheer et al. (2012), with permission from Springer Nature Customer Service Center (SNCSC). Fi, filtrate; GR, gill raker; MF, mainstream flow.

location, and function. For example, the particle separator (a) required that the investigator inject an annulus of particle-free water to encircle the entering flow as a "shield" to reduce the loss of particles through slits along the sides of the device, and (b) relied on particle accumulation and collection using suction through a tube connected to a hole in the bottom of the device approximately halfway between the device's anterior and posterior (Hung et al., 2012; Hung and Piedrahita, 2014). The highest particle removal efficiency achieved in experiments using a physical model of this separator was approximately 43% (particle diameter 500 µm, density 1050 kg m^{-3}; Hung and Piedrahita, 2014).

5.5 Cross-step filtration

Obstacles as diverse as rocks in a river, automobiles, and buildings form backward-facing steps that generate downstream vortices (Chen et al., 2018; Montazer et al., 2018). In CFD simulations and flow tank experiments with physical models using the crossflow configuration, the BAs and GRs acted as backward-facing steps that generated a vortical recirculation zone when flow separation (not to be confused with particle separation) occurred at the downstream edge of each step (Figure 9) (Sanderson et al., 2016; Van Wassenbergh and Sanderson, 2023; Witkop et al., 2023; Xu et al., 2023). As flow travels over each step, a trapped vortex forms directly downstream near the step due to the sudden expansion of cross-sectional area in the channel there (Chen et al., 2018).

A series of backward-facing steps forms a rib-and-groove arrangement, with the BAs and/or GRs in SF fishes serving as rib-shaped structures and the grooves between them serving as the slots through which filtrate exits past the trapped vortex in each slot (Figure 9, Sanderson et al., 2016; Storm et al., 2020). Therefore, BAs and GRs differ from backward-facing steps that are found commonly in heat exchangers, petroleum pipe-flow transport systems, and other industrial applications (Salman et al., 2020; Hong et al., 2021) because the floor of the slots between the steps (i.e., the floor of the groove between the ribs in industrial applications) is not solid in fish. A major distinction between slots versus most pores or meshes is that a slot is a three-dimensional structure with height as well as width and an elongated length. The slot aspect ratio (slot width divided by rib height, Figure 9D) is a key design metric affecting the fluid dynamics, including the vortical flow, in cross-step systems (e.g., Stel et al., 2012; Sanderson et al., 2016; Schroeder et al., 2019; Xu et al., 2023).

Based on flow tank experiments using American paddlefish specimens (*Polyodon spathula*) that had been preserved in ram SF position and 3D-printed physical models of paddlefish oral cavities, Sanderson et al. (2016) proposed vortical cross-step filtration as a novel particle separation mechanism (Figure 9A). By broadening the CFD simulations of Sanderson et al. (2001) and Cheer et al. (2006, 2012) to three dimensions in a flow tank, Sanderson et al. (2016) demonstrated how trapped vortices could suspend, concentrate, and transport particles in the slots between the BAs of paddlefish and basking sharks (Figure 9B). In these two species, the GRs have evolved convergently to form the porous floors of the deep slots between the BAs. In the flow tank experiments, a mesh was used to simulate the GRs on the floors of the deep slots between BAs. As filtrate exited through the mesh between the BAs in the preserved paddlefish and the physical models, the flow that had separated at the downstream edge of each BA wrapped around the trapped vortex inside each slot. This separated flow, known as a shear layer, caused a high shear rate along the surface of the mesh (Van Wassenbergh and Sanderson, 2023) and thereby transported particles (~ 250 µm diameter) to the margins of the slots (Sanderson et al., 2016). Transport of concentrated particles to the esophagus was hypothesized to occur via the ceratobranchial-epibranchial junctions, but was not modeled. The Reynolds number was ~ 600, calculated using the mainstream flow speed (10 cm s^{-1}) and the height of the backward-facing step.

Vortical cross-step filtration reduces clogging by causing a high shear rate along the filter surfaces downstream of each backward-facing step (Sanderson et al., 2016; Xu et al., 2023). Vortical cross-step filtration has been hypothesized to operate in SF clupeids (e.g., herring, menhaden, shad) and engraulids (anchovies), with the denticles on the GRs proposed to serve as the porous filter surfaces inside the slots between the backward-facing steps formed by the GRs (Sanderson et al., 2016; Storm et al., 2020).

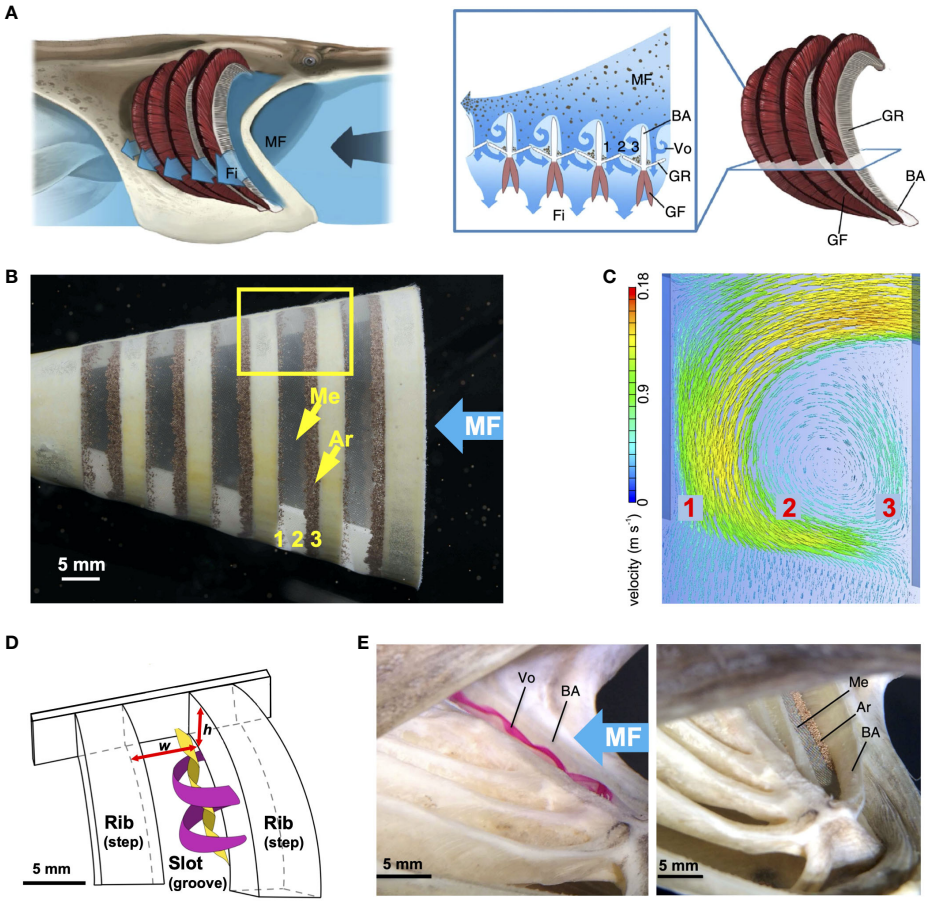

FIGURE 9
Vortical cross-step filtration has been proposed to generate trapped vortices that could suspend, concentrate, and transport particles in the slots between the branchial arches and gill rakers of SF fishes (Sanderson et al., 2016; Storm et al., 2020; Van Wassenbergh and Sanderson, 2023). **(A)** Illustration of cross-step filtration proposed in paddlefish, with BAs acting as backward-facing steps to generate vortical recirculation that concentrates particles in zones 1 and 3 along the slot margins. **(B)** 3D-printed model in flow tank experiments with 140-µm mesh simulating the paddlefish GRs by covering the exterior of the slots between BAs (Re ~ 600). Particles (*Artemia* cysts, ~ 250 µm diameter) were concentrated in zones 1 and 3 of the slots, while vortical flow reduced clogging in zone 2. **(C)** CFD simulation of vortical flow in slots of model used for flow tank experiments. **(D)** Enlargement of yellow rectangle from **(B)**, showing a series of backward-facing steps with a slot between each pair of steps, forming a rib-and-groove arrangement with slot width *w* and rib height *h*. Representative locations of outer (magenta) and inner (yellow) path lines of the vortical flow were obtained from flow tank experiments. **(E)** Vortical flow and particle concentration in paddlefish preserved in SF position in a flow tank, with mesh simulating the GRs which do not abduct in dead specimens. **(A)** © Virginia Greene/virginiagreeneillustration.com, used with permission, not covered by the CC-BY license. **(B, E)** adapted from Sanderson et al. (2016), CC BY 4.0. **(C)** adapted from Van Wassenbergh and Sanderson (2023), CC BY 4.0. **(D)** adapted from Brooks et al. (2018), CC BY 4.0. Ar, *Artemia* cysts; BA, branchial arch; Fi, filtrate; GF, gill filament; GR, gill raker; *h*, rib height; Me, mesh; MF, mainstream flow; Vo, vortex; *w*, slot width.

Schroeder et al. (2019), Masselter et al. (2023), and Xu et al. (2023) have applied vortical cross-step filtration to construct filters with reduced clogging for harmful algae collection, washing machines, and drip-irrigation systems, respectively. In their physical models, vortices generated in the slots between ribs served to reduce clogging by transporting particles to the margins of the slots. They did not quantify particle removal efficiency because the objective of the cross-step designs was to reduce clogging. From their CFD simulations, Xu et al. (2023) determined that approximately 10 - 18% of the particles retained by the mesh in the slots were trapped in the region scoured by the shear layer downstream from each step, demonstrating that the shear layer was effective in reducing clogging. However, with continued use, the cross-step filters of Schroeder et al. (2019) clogged eventually unless active anti-clogging strategies were introduced (i.e., perturbation of the physical model by tapping or by rotation of the model). The physical models of Schroeder et al. (2019) differed from SF fishes by using helical slots that reduced clogging by enabling the transport of particles to the open posterior end of the model, following resuspension of the particles by tapping or by rotation of the model.

5.6 Vortical flow along outer faces of gill raker plates in silver carp

Cohen et al. (2018) used 3D particle image velocimetry in flow tank experiments to quantify flow past 3D-printed physical models based on micro-CT scans of the GRs in silver carp and bighead carp. In silver carp, the highly modified GRs form specialized filtering plates

(Figure 10A) (Cohen and Hernandez, 2018). Physical models of the silver carp GR plates (Figure 10B) induced a strong organized vortical flow on the outer faces of the plates (Figure 10C) at Re ~ 18,000 (calculated using a flow tank speed of 15 cm s^{-1} and the downstream length of the filtering plates that had been scaled to match the Re for a silver carp body length of 80 cm and a flow speed of 0.75 body lengths s^{-1}). Cohen et al. (2018) hypothesized that the vortices increased the number of interactions between the particles and pores inside the channels on the outer faces of the silver carp filtering plates, leading to particle transport through the pores and subsequent accumulation at the inner faces of the plates. Because the physical models of the less modified GRs in the bighead carp induced only limited disorganized vortices, they suggested that bighead carp use a haphazard crossflow filtration which could be related to decreased filtration efficiency on small particles relative to silver carp (Cohen et al., 2018).

5.7 Ricochet filtration

Manta rays and devil rays (*Mobula*, Mobulidae) have a specialized SF apparatus with highly modified GRs consisting of arrays of lobes attached to the chevron-shaped BAs (Figure 11A). The lobes are arranged in two sets of filter plates, one oriented anteriorly and the other oriented posteriorly (Paig-Tran et al., 2013). Based on two-dimensional CFD simulations and 3D-printed models of the lobe arrays that were tested in a customized flume, Divi et al. (2018) reported that ricochet filtration is a novel particle separation mechanism in manta rays that does not resemble previously described filtration systems. Their computational and physical models used morphological measurements of the lobe arrays in *M. birostris* as well as micro-CT scans of *M. tarapacana*. For *M. birostris*, the Re was 1075, calculated using the freestream velocity estimated for the buccal cavity of a freely swimming manta ray (55 cm s^{-1}) and the distance between lobes.

Based on the orientation of the filter plates within the oral cavity, Divi et al. (2018) suggested that water impinges on the lobes in both the forward direction ("wing-like" posterior filters) and the reversed direction ("spoiler-like" anterior filters) (Figures 11B, C). As water traveled across the wing-like or spoiler-like lobes in the models, flow separation occurred behind the leading edge of each lobe and a captive vortex was generated directly downstream inside the pore between two consecutive lobes (Figure 11D).

In the CFD simulations, fluid streamlines immediately above the lobes entered the pores and were swept around the captive

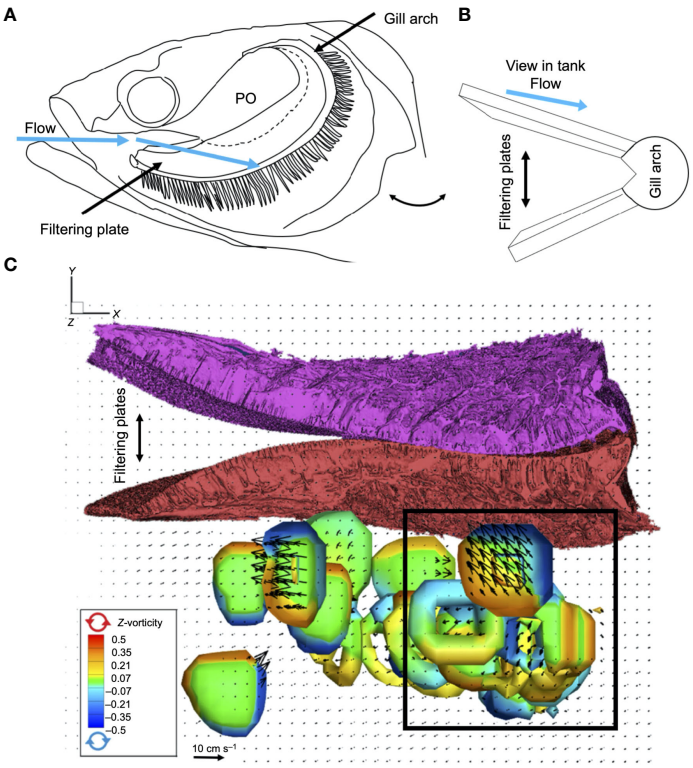

FIGURE 10
Vortical flow quantified along the outer faces of 3D-printed physical models of silver carp (Cyprinidae) filtering plates using 3D particle image velocimetry in a recirculating flow tank (Cohen et al., 2018). **(A)** Orientation of filtering plates in crossflow inside the oral cavity. **(B)** Orientation of physical model during flow tank experiments, with flow moving across the model in an anterior to posterior direction from the dorsal edge of the filtering plates to the ventral base of the gill arch. **(C)** Particle volumetric data from the flow tank speed (0.75 body lengths s^{-1}) that developed and maintained strong, organized vortical flow (bottom) across the outer faces of the filtering plates (top). Black box denotes region where vortices changed direction such that vortical flow was in the direction of the epibranchial organ, traveling through channels along the outer faces of the filtering plates. Adapted with permission of The Company of Biologists Ltd from Cohen et al. (2018), permission conveyed through Copyright Clearance Center, Inc. PO, palatal organ.

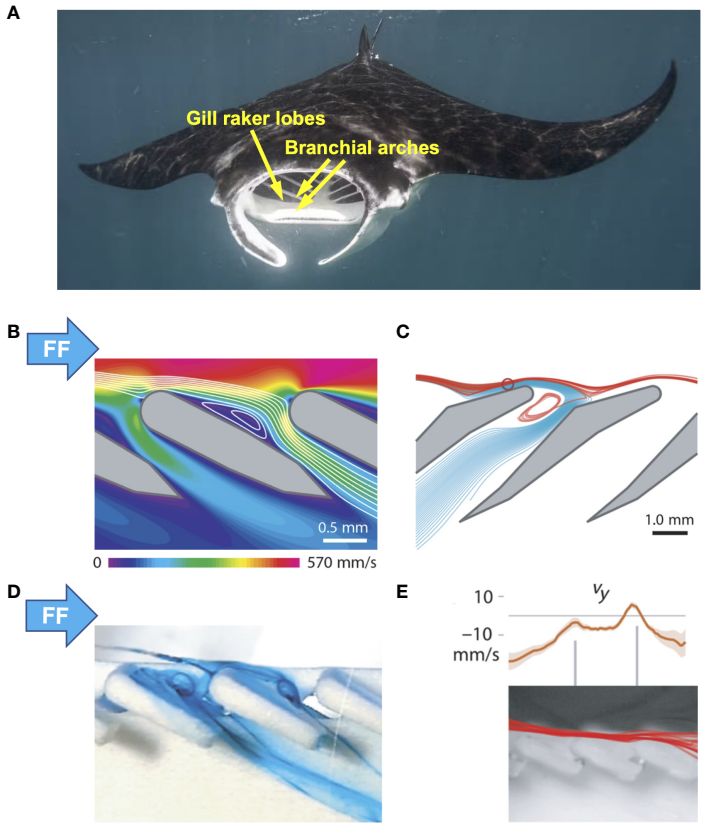

FIGURE 11
Ricochet filtration has been proposed by Divi et al. (2018) as a unique nonclogging particle separation mechanism operating in the highly modified gill raker lobes of ram SF manta rays (Mobulidae). **(A)** Unlike in bony fishes, water in the buccal cavity of mobulids must make an abrupt 90° turn to reach the rows of GR lobes that extend dorso- and ventro-laterally between the branchial arches. *Mobula alfredi*, © Edy Setyawan, modified and used with permission, not covered by the CC-BY license. **(B)** CFD simulation of flow speed and streamlines along and between *Mobula birostris* GR lobes in the wing-like orientation (Re = 990). Water forms a thin boundary layer on the upstream surface of each lobe and passes around a large, captive vortex in the pore between consecutive lobes before exiting as filtrate. **(C)** CFD simulation of fluid streamlines (blue) and particle trajectories (350 µm diameter; neutrally buoyant; center of mass, red) as they pass over *Mobula tarapacana* lobes in the spoiler-like orientation (Re = 1115). Particles (e.g., dark red outline) encounter the tips of the lobes by direct interception. Consequently, solid-liquid separation occurs as contact forces cause particles to recoil elastically from the lobe surface and ricochet back into the faster freestream flow, deviating from the fluid streamlines that pass through the filter pore. **(D)** Dye injection in flow tank experiments with physical models at 4x scale to visualize fluid pathlines around *M. birostris* lobes in the wing-like orientation (Re = 745), for comparison with **(B)**. **(E)** Trajectories (red) of *Artemia* cysts passing over physical models of *M. birostris* lobes in the wing-like orientation at 1x scale (Re = 309) in flow tank experiments. Increases in the vertical velocity of particles corresponded to the location of the leading edge of each lobe. **(B–E)** adapted from Divi et al. (2018), © the Authors, some rights reserved; exclusive licensee AAAS. **(B–E)** distributed under a CC BY-NC 4.0 license http://creativecommons.org/licenses/by-nc/4.0/. **(B–E)** reprinted with permission from AAAS. FF, freestream flow.

vortex prior to exiting as filtrate from the pores (Figures 11A, B) (Divi et al., 2018). However, particles (~ 200 – 800 µm diameter) deviated from these streamlines and did not enter the pores (Figure 11E). Instead, particles encountered the leading edge of the lobes by direct interception. The CFD simulations indicated that contact forces caused particles to recoil elastically from the lobe surfaces (i.e., "ricochet" away from the pores), thereby concentrating the particles in the water above the lobes. Divi et al. (2018) concluded that ricochet filtration in mobulid rays is a unique nonclogging filtration mechanism that operates at high flow rates and effectively filters particles with densities ranging from 950 to 1100 kg m^{-3}. Unlike the physical principles of deterministic lateral displacement (see critical separation radius and stagnation streamline discussed in section 5.8 below), ricochet separation involves contact forces that cause particles to recoil elastically (i.e., ricochet) from uniquely structured lobe surfaces.

Adelmann et al. (2022) applied ricochet filtration to design either flat filters or cylindrical filters that could be employed in hoses and pipe systems as precipitators for sand. Their cylindrical design differed from the relatively flat filter plates of manta rays. The highest precipitator efficiency of > 95% was achieved in experiments using the cylindrical "spoiler-like" arrangement (sand diameter ~ 240 µm; Adelmann et al., 2022).

5.8 Lateral displacement

Deterministic lateral displacement arrays, termed "bump arrays", of staggered obstacles (e.g., microposts) were discovered by Huang et al. (2004) and are used today in microfluidics and mesofluidics for the size separation of particles at gap Re ranging from 10^{-3} to 10^{3} and particle sizes from submicron to millimeters

(Hochstetter et al., 2020; Burns et al., 2021). In deterministic lateral displacement devices and similar sieve-based lateral displacement arrays in crossflow (Dijkshoorn et al., 2018), the physical principle that results in particle separation is that particles with a radius larger than the critical separation radius are repeatedly displaced laterally across streamlines (i.e., are "bumped") upon direct interception with the obstacles, whereas smaller particles follow streamlines (Salafi et al., 2019; Pease et al., 2022). The critical separation radius is determined by the specific geometry and operating parameters of each lateral displacement array, and is identified with reference to the stagnation streamline that terminates on each obstacle (Hochstetter et al., 2020).

Witkop et al. (2023) conducted flume experiments with conical physical models that had 3D-printed arrays of generalized GRs (gap Re 260 – 350, calculated using the flume speed of 19.3 cm s^{-1} and the slot width of 1.35 or 1.8 mm, scaled to match the swimming speed and GR dimensions from SEMs of the ram SF American shad, *Alosa sapidissima*, Clupeidae) (Figures 12A, B). To approximate the value of the critical separation radius at each GR (i.e., obstacle) using CFD simulations and the principles of deterministic lateral displacement, the streamline that terminated at the stagnation point on each GR was traced back to the location where that streamline passed over the GR immediately upstream in the array (Figure 12C). The shortest distance between that "dividing streamline" (i.e.,

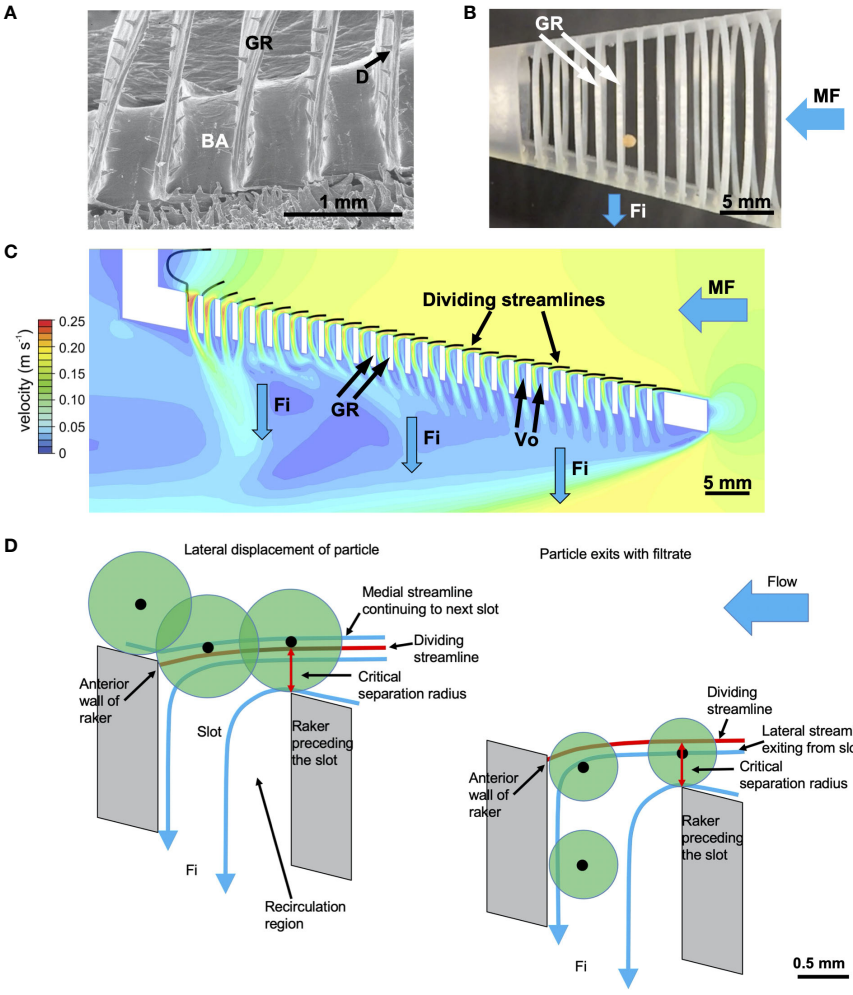

FIGURE 12
The gill rakers of SF fishes have been proposed by Witkop et al. (2023) to function using the principles of lateral displacement arrays for the size separation of particles in microfluidics and mesofluidics. **(A)** SEMs of GRs on the BAs of ram SF American shad (Clupeidae) were the basis for the design of generalized models. **(B)** 3D-printed conical models were used in flume experiments to quantify particle exit from each slot between adjacent GRs (gap Re 260 – 350). **(C)** CFD simulations of flow patterns in the conical physical models were used to quantify the location of each dividing streamline (i.e., stagnation streamline). **(D)** Schematic illustration of particle separation that was recorded in the flume experiments using the physical models. Statistical analyses supported the hypothesis that the shortest distance between the dividing streamline and the surface of the preceding GR predicts the maximum radius of a particle that will exit from the physical model by passing through that slot in the flume experiments. This theoretical maximum radius is analogous to the critical separation radius in microfluidic and mesofluidic devices that use deterministic lateral displacement and sieve-based lateral displacement for the size separation of particles. **(A–D)** adapted from Witkop et al. (2023), CC BY 4.0. BA, branchial arch; D, denticle; Fi, filtrate; GR, gill raker; MF, mainstream flow; Vo, vortex.

stagnation streamline) and the surface of the preceding GR was identified as the maximum radius of a particle that would exit through the gaps between GRs (Van Wassenbergh and Sanderson, 2023; Witkop et al., 2023, Figure 12D).

In the immediate vicinity of the GRs, particles that were smaller than the gap between GRs but had a radius larger than the critical separation radius skipped over the trapped vortex that was generated downstream from each GR and then approached the surface of the subsequent GR (Figure 12D, left). Because the center of these particles was located medial to the dividing streamline (i.e., closer to the interior of the model), these particles deviated from streamlines as they were displaced toward the interior of the model and then continued to travel toward the posterior of the model. This lateral displacement of particles with a radius larger than the critical separation radius is called "deterministic" because the specific locations of the dividing streamlines constrain the center of these particles to be displaced closer to the interior of the model.

Particles that had a radius smaller than the critical separation radius exited with the filtrate through the gaps between GRs (Figure 12D, right). The hypothesis predicting the exit of particles based on mass flow rates, the critical separation radius as determined by the location of the dividing streamlines, and particle size was supported by the results of the flume experiments, indicating that the physical principles of lateral displacement arrays can be applied to the design of biomimetic models based on the gill rakers of SF fishes (Witkop et al., 2023).

This functional analogy between lateral displacement arrays and the arrangement of SF fish filter elements provides new perspectives and metrics for exploring particle separation in SF fishes and lateral displacement arrays (Witkop et al., 2023). Further research is needed to determine whether lateral displacement systems in SF fishes are dependent on the contact forces modeled in ricochet filtration by Divi et al. (2018), and whether ricochet filtration in manta rays and devil rays is dependent on the critical separation radius identified in lateral displacement systems with reference to the stagnation streamline (e.g., Hochstetter et al., 2020).

5.9 Multiple or hybrid mechanisms within species

Experiments are needed to determine whether species use multiple or hybrid particle separation mechanisms during suspension feeding. Very limited data are available to address whether SF fishes exhibit intra-individual variation in particle separation mechanisms depending on fish ontogenetic stage and on prey size, density, etc. (e.g., Sanderson et al., 1996b; Callan and Sanderson, 2003), and no experiments have tested for inter-individual variation within species. Because four of the eight particle separation mechanisms discussed here for SF fishes have been proposed within the past ten years only, the potential for hybrid mechanisms that combine morphological and functional aspects of more than one mechanism has not been explored. The possibility of multiple or hybrid particle separation mechanisms within SF fish species has important ecological and evolutionary implications, particularly if the composition of prey species is in flux due to environmental changes, and warrants study.

6 Retention of particles smaller than the pore sizes

Researchers have been particularly interested in the retention of particles that are smaller than the pore sizes between the filter elements in SF fishes. Such retention may characterize the occurrence of novel particle separation mechanisms that do not involve the accumulation of particles on the filter elements and that could therefore reduce clogging. The rationale is that, if a non-adhesive filter can evolve or can be designed by a filtration engineer to separate particles that are smaller than the pore size, then such a filter should retain the targeted particles (i.e., the desired particles of interest) with minimal clogging.

However, primary literature articles that have been cited previously as supporting the retention of particles smaller than the pore sizes in SF fishes have often been studies of species that were particulate feeding on individual prey rather than SF, species for which pore measurements were made on the first BA only, and/or species in which the prey sizes that were retained were larger than the pore sizes (e.g., Seghers, 1975; Wright et al., 1983; Langeland and Nøst, 1995). In one of the clearest examples of the retention of particles smaller than the pore sizes, Friedland et al. (2006) noted that transitional juvenile Atlantic menhaden showed significant particle retention at a threshold just below 10 μm (Friedland et al., 1984), despite minimum pore sizes of approximately 16 μm between the branchiospinules. Friedland et al. (2006) commented that potential explanations for this discrepancy include a reduction in the effective pore size when particles are crowded on the branchial sieve (Friedland et al., 1984), and/or the retention of particles due to other mechanisms such as those involving crossflow filtration.

As discussed earlier, entrapment in mucus on filter element surfaces in Nile tilapia has been observed endoscopically to result in the capture of particles that can be much smaller than the pores between the filter elements (Sanderson et al., 1996b). Even when SF fishes such as menhaden retain particles that are smaller than the pores, mucus entrapment can be rejected as a particle separation mechanism if mucus cells are not located on the filter elements, as has been documented for Atlantic menhaden branchiospinules (Friedland, 1985) and basking shark GRs (Paig-Tran and Summers, 2014; Surapaneni et al., 2022). Mucus has also been rejected as a particle separation mechanism when endoscopic observations have indicated that mucus does not trap particles during feeding in specific species (e.g., ngege tilapia, Goodrich et al., 2000). However, in all these cases, mucus secreted by cells on other oral surfaces could still be involved in particle aggregation and transport toward the esophagus, as hypothesized for basking sharks (Matthews and Parker, 1950; Sanderson et al., 2016).

The most puzzling example of the retention of particles smaller than the pore sizes was reported by Drenner et al. (1987) for the Galilee Saint Peter's fish or mango tilapia (*Sarotherodon galilaeus*,

Cichlidae) following surgical removal of the GRs and microbranchiospines. Comparable results were reported subsequently by Smith and Sanderson (2007, 2008, 2013) for two related SF cichlid species. Microbranchiospines are denticulate projections (~ 150 μm length) arranged in a row on the BAs of most SF and non-SF species in the family Cichlidae, for which the function is uncertain (Beveridge et al., 1988). Fish that had only partially regenerated the GRs and microbranchiospines on the healed BAs nonetheless retained large numbers of microspheres (20 – 70 μm in diameter) while feeding on zooplankton. The surgical procedure did not affect particle ingestion rates or size selectivity of microspheres (Drenner et al., 1987).

In experiments with two species that are closely related to *S. galilaeus* (*Oreochromis aureus*, blue tilapia, and *O. esculentus*, ngege tilapia, Cichlidae), Smith and Sanderson (2007, 2008, 2013) modified the experimental protocol of Drenner et al. (1987). The procedures were refined by ensuring that the healed BAs were smooth without regeneration of GRs and microbranchiospines, by confirming with a fiberoptic endoscope that mucus was not visible and that particles were not retained on the BAs during crossflow filtration, and by measuring and counting microspheres in all fecal strings to quantify particle retention. Surgical removal of all GRs and microbranchiospines in these two tilapia species affected particle size selectivity in *O. esculentus* but did not significantly affect the total number of particles (11 – 200 μm diameter) retained by either species. Both species continued to selectively ingest particles > 50 μm. Interestingly, after the surgery, *O. esculentus* retained significantly more microspheres 51 – 70 μm in diameter and significantly fewer microspheres 91 – 130 μm in diameter compared to retention with intact oral structures (Smith and Sanderson, 2013). The continued size selectivity and the decreased retention of larger particles following removal of the filter elements suggests that particle separation mechanisms such as inertial lift, shear-induced migration, or lateral displacement may have occurred at the level of the BAs themselves.

7 3D movement of gill rakers and associated protrusions

Despite the critical importance of the pore sizes between filter elements, there have been very few studies on the extent and control of the three-dimensional movement of GRs and associated protrusions during SF. Although BA and GR abduction during mouth opening can be observed readily *in vivo* in multiple taxa of SF fishes, the functional morphological mechanisms that control the erection, rotation, and spreading of GRs on the BAs in SF and non-SF fishes have been investigated rarely (e.g., Matthews and Parker, 1950; Kirchhoff, 1958). Consequently, data are not available to describe and explain the apparent ability of the GRs on the BAs of many SF and non-SF fishes to move during BA abduction as the mouth is opened. Such GR movements can be observed readily in many taxa by manually manipulating freshly dead specimens to cause abduction of the BAs. Further study is a high priority, because the specific 3D orientations of the GRs relative to the approaching flow while the mouth is opened and closed and the BAs are abducted and adducted, as well as concomitant changes in the sizes and shapes of the gaps between GRs, are key for further progress in modeling fish SF.

Paddlefish and basking sharks have evolved convergent morphology consisting of long, thin GRs attached to the anterolateral and posteromedial margins of deep slots formed by the BAs (Sanderson et al., 2016). During ram SF *in vivo*, the GRs of both species can be observed to abduct and extend across much of each slot between adjacent BAs. However, unlike the case in many other SF fish species, the GRs in freshly dead paddlefish specimens lie relatively flat against the BAs rather than erecting passively when the BAs are abducted by manual manipulation. This suggests that GR abduction in paddlefish may be caused actively (e.g., by muscle contraction) or passively (e.g., by water pressure).

Imms (1904) and Matthews and Parker (1950) described muscle fibers as well as elastic fibers attached to the basal part of each GR, connecting the base of the GR to the BA in paddlefish and the basking shark, respectively. Both suggested that contraction of these muscle fibers could pull the GRs away from the sides of the BAs during SF, whereas the elastic fibers could return the GRs to lie flat on the BAs. However, unlike Imms (1904), Matthews and Parker (1950, p. 565) suggested that elastic fibers in a band of connective tissue connecting the bases of the basking shark GRs could serve to maintain GR position "against the pressure of the gill current", and could subsequently return the GRs to their resting position flat on the BA surfaces when the mouth had closed and the pressure had ceased. In what appears to be the only report for bony fishes, Kirchhoff's (1958) extensive study on the functional morphology of the herring (*Clupea harengus*, Clupeidae) included a detailed description of a hypothesized mechanism for GR movement in three dimensions during SF. In contrast to the proposed mechanisms for paddlefish and basking sharks, Kirchhoff (1958) suggested that stretching of an elastic band connecting the GRs along the BA was responsible for GR abduction and rotation during mouth opening and BA abduction.

In a comprehensive assessment of teleost striated muscles, Winterbottom (1974) described minute muscles called interbranchiales abductores connecting the respiratory gill filaments to the lateral faces of the BAs. He noted that these muscle fibers may become "intimately associated" with the GRs, especially in species with well-developed GRs, and he illustrated the interbranchiales abductores attaching to the filaments and to the bases of the GRs in a planktivorous deep-sea fish (Winterbottom, 1974, p. 261). Springer and Johnson (2004) referred to "gill filament muscles" that they considered to be essentially the same as the interbranchiales abductores, and noted that these fine muscles could be obscured by or fused with adductor muscles on the BAs that attach the epibranchial to the ceratobranchial. They recommended additional study of these adductors and gill filament muscles. The extent to which any of these muscles are thought to cause gill filament and GR movement is not clear.

Using histological sections of the BAs of SF common bream (*Abramis brama*, Cyprinidae), Hoogenboezem et al. (1991) identified a complex of minute muscles connecting the bases of the lateral GRs to the BA. Using X-ray cinematography, they observed that zooplankton prey to which a 1-mm iron sphere had

been glued were retained between adjacent BAs. They proposed a reducible-channel model of branchial sieve adjustment in which muscles could retain particles by moving the tips of lateral GRs into the channels between the medial GRs. Subsequently, van den Berg et al. (1994b) revised the names and functions of the muscles in this complex and expanded the application of the reducible-channel model to carp (*Cyprinus carpio*, Cyprinidae). Vandewalle et al. (2000) addressed the discrepancies between these earlier reports and summarized the most recently proposed names, locations, and functions of these muscles. However, the functional morphology of these muscles and their ability to control GR movement do not appear to have been explored subsequently in the primary literature on SF or non-SF species (e.g., Hoogenboezem, 2000; Sibbing and Nagelkerke, 2001; Presti et al., 2020). Endoscopic videotapes of SF *Cyprinus carpio* did not record GR movements that were independent of BA movements (Callan and Sanderson, 2003).

Similarly, the potential for active or passive movement of denticles and other protrusions on the GRs is virtually unstudied. For example, in specimens of Pacific sardine (*Sardinops sagax*, Clupeidae) and northern anchovy (*Engraulis mordax*, Engraulidae) that had been frozen and subsequently thawed, Rykaczewski (2009) noted under a light microscope that the denticles on the GRs deflected passively at their bases in response to water pressure, abducting to extend toward the adjacent GR. Thus, there is an urgent need for research on active or passive movements of GRs and associated protrusions during SF in multiple taxa.

Fortunately, the functional, morphological, and biomechanical mechanisms that are responsible for BA abduction and the 3D expansion of fish oral cavity volume during feeding have been well studied using innovative approaches (e.g., Camp et al., 2015; Kenaley and Lauder, 2016; Olsen et al., 2020). In addition, techniques and equipment for the 3D reconstruction, visualization, and manipulation of complex and dynamic biological structures are advancing rapidly (Irschick et al., 2022). Such research provides a wealth of knowledge on which future progress in our understanding of 3D movements of the BAs and oral cavity during SF can build. For example, a new shape space-based approach for estimating complex 3D shapes from single monocular 2D images is being developed to create 3D skeletal representations of the basking shark head (Paskin et al., 2022). The ultimate goal of that work is to enable a 3D reconstruction of the head skeleton, including identification of the skeletal joint locations, from a 2D image of a basking shark oral cavity during SF (Paskin et al., 2022). This is valuable because 2D images of ram SF oral cavities can be obtained relatively easily *in vivo*.

8 Unidentified SF fish taxa, diets, and particle separation mechanisms

8.1 Unidentified SF fish taxa

At present, whether a fish species has been identified as a suspension feeder is based primarily on whether the species has been observed to exhibit either pump or ram SF behavior, and/or whether minute particles such as phytoplankton are abundant in the gut. For these reasons, at least three genera of SF fishes in a non-SF family were reported to have been overlooked previously (*Seriola*, *Pseudocaranx*, *Oligoplites*, Carangidae, Sanderson et al., 1996a; Sazima, 1998), and other species, genera, and even families of SF fishes may remain yet unrecognized. Such oversights are of concern because the GRs of non-SF fish species are generally assumed to serve simply as barriers that block the exit of large particles between the BAs and thereby protect the gill filaments. The intraoral morphology and fluid dynamics of non-SF species have not been evaluated from the perspectives of the types and sizes of particles that might be retained during SF processes. Therefore, species that have been assumed to be solely particulate feeders might obtain ecologically important dietary components from the non-selective retention of suspended particles, particularly species that are also ram ventilators (e.g., scombrids such as tuna, Magnuson and Heitz, 1971; Estrada et al., 2005).

8.2 Particle retention by non-SF fish species

Sanderson et al. (1998) quantified the retention of suspended polystyrene microspheres (31 – 90 μm diameter) and brine shrimp cysts (210 – 300 μm diameter) by two non-SF cyprinid species (insectivorous Sacramento squawfish, *Ptychocheilus grandis*; omnivorous benthic-feeding California roach, *Hesperoleucus symmetricus*) in the presence of finely crushed Tetramin flakes or dead adult brine shrimp. Although SF behavior was not observed during the experiments and electron microscopy of these species did not show unique intraoral morphology, the large number of brine shrimp cysts quantified in the fish feces after 10 minutes of exposure to the particles was equivalent to the amount in a volume of aquarium water that was 1 - 15 times the fish body volume. In addition, small numbers of microspheres were excreted in the fecal strings. The brine shrimp cysts were large enough to have been trapped between GRs, while both the brine shrimp cysts and microspheres could have been retained on mucus-covered oral surfaces. Sanderson et al. (1998) concluded that non-SF fish species may routinely retain small suspended particles during particulate feeding on larger prey or during ventilation, and noted that there could be ecological and ecotoxicological implications (as evidenced recently for microplastics, e.g., De Sales-Ribeiro et al., 2020).

8.3 Retention of detritus in SF fishes

The potential retention of detritus is another case in which dietary components of SF and non-SF fishes might not be recognized fully. Detritus refers broadly to aggregates of organic material consisting of dead plankton, decaying vascular plant material, fecal pellets, microbes, etc. In marine environments, similar aggregates have also been termed “marine snow” (Turner, 2015). Detritus appears in the gut of Atlantic menhaden as unidentifiable amorphous material (Lewis and Peters, 1994)

which has relatively low nutritive value compared to zooplankton and phytoplankton but can comprise a significant fraction of the juvenile menhaden diet (Annis et al., 2011). Juveniles of two pump SF mullet species ingested marine snow in laboratory experiments (*Mugil curema*, *M. cephalus*, Mugilidae, Larson and Shanks, 1996). Research is needed to determine whether other SF species as well as non-SF species also ingest suspended detritus and marine snow, as this could impact ecosystem energy budgets and nutrient cycles.

8.4 Oil-water separation mechanisms in fishes

Oil-water separation mechanisms, which could be either solid-liquid or liquid-liquid separations depending on temperature, warrant study in SF fishes. A number of SF fish species can protrude the dorsal portion of their oral jaws above the surface of the water, and either swim the open mouth forward around the surface layers (ram SF) or suck the surface layers into the oral cavity (pump SF). Ram SF fishes have been reported to swim forward with their open jaws in this position (e.g., whale shark, *Rhincodon typus*, Motta et al., 2010; manta ray, *Mobula birostris*, Paig-Tran et al., 2013), whereas pump SF fishes can remain stationary or swim forward slowly while pumping the surface layers into their oral cavity (e.g., goldfish, Edwards et al., 2017). Bighead carp have been reported to use both ram and pump SF to engulf surface layers of water (Kolar et al., 2007).

In laboratory experiments, untrained goldfish used pump SF behavior to feed voluntarily on liquid canola oil in a layer on the surface of the water in the aquarium (Edwards et al., 2017). Nine of 15 individuals swallowed oil that was quantifiable in the gut using fatty acid methyl ester (FAME) preparations for gas chromatography-mass spectrometry (GC-MS) analysis. Whereas control fish that were in aquaria without access to the oil on the water surface had no detectable oil in their guts, fish with access to the surface swallowed 0.01% - 14% of the 2.0 ml of oil present in the aquaria during the 20-minute experiments. SF goldfish in manmade outdoor ponds also exhibited pump SF behavior at the pond surface in response to vegetable oils that had been added to the surface (Edwards et al., 2017). In laboratory experiments, zooplankton and barnacles use their appendages to capture edible as well as crude oil droplets up to ~ 10 μm diameter (Letendre et al., 2020; Letendre and Cameron, 2022). Mechanisms by which SF fishes might retain surface films, suspended droplets, or floating globules of hydrophobic organics have not been investigated, although crossflow membrane filtration and hydrocyclones are major technologies for separating oils from wastewater (e.g., Nunes et al., 2021; Su et al., 2021; Yang et al., 2022).

Natural slicks at the air-sea interface can cover up to ~ 80% of the surface during calm weather conditions in coastal marine areas. Recent data indicate that natural slicks often have high organic matter content, composed primarily of biosurfactants produced by bacteria and by micro- and macroalgae (review by Voskuhl and Rahlff, 2022). In the sea-surface microlayer, these polymeric materials orient according to their hydrophobic constituents (e.g., glycolipids, lipopeptides, and fatty acids) versus hydrophilic constituents (Ron and Rosenberg, 2001).

Thus far, the potential abilities of SF fishes and continuous skim-feeding balaenid whales to separate and ingest the hydrophobic organics in natural slicks and/or ingest zooplankton associated with surface slicks are unknown. However, Couturier et al. (2013a, 2013b) noted that signature fatty acid analyses of tissue from whale sharks and the reef manta ray *Mobula alfredi* raised questions about the origin of their primary food source, suggesting the importance of both pelagic and demersal zooplankton. Recently, the fatty acid profiles of whale shark tissues and feces were identified as being most similar to those of the floating macroalgae *Sargassum*, leading Meekan et al. (2022) to suggest that whale sharks are omnivores that consume *Sargassum* fronds and associated epibionts. To date, the potential roles that naturally occurring surface films and droplets of hydrophobic organics (such as might be produced by the degradation of *Sargassum*) might have in the diet of SF fishes, and the particle separation mechanisms that could be used, remain virtually unstudied (Edwards et al., 2017).

9 Conclusions and challenges

This comprehensive synthesis has assessed our knowledge of particle separation mechanisms in SF fishes, related recent developments to industrial, commercial, and biomedical separation processes and applications, identified critical gaps in our understanding and approaches, and offered perspectives on future research priorities. Recent research has led to transformational discoveries in the fluid dynamics and biomechanics of filter element function in SF fishes. Particle separation mechanisms in SF fishes are not limited to dead-end filtration through porous filter media or mucus entrapment on an adhesive filter. Of the eight particle separation mechanisms for SF fishes presented here, six have been proposed since 2001.

Although substantial progress has been made over the past three decades in understanding the ecological, morphological, and functional complexity of fish SF, important unresolved questions vastly outnumber answers. A major goal continues to be the identification of patterns and unifying principles for particle separation across the breadth of SF fish taxa, morphology, ecology, and function (e.g., patterns of evolutionary convergence or divergence related to facultative versus obligate SF, pump versus ram; Reynolds numbers; dietary particle size, shape, density, and concentration). Challenges in this endeavor will be the diversity of SF fishes and the likely operation of multiple or hybrid particle separation mechanisms within species. As discussed here, unidentified SF fish taxa, diets, and particle separation mechanisms await discovery, including the potential separation of hydrophobic films and droplets by SF fishes.

During the past twenty years, transformational research in filtration engineering has also opened entirely new directions for particle manipulation and separation, such as inertial microfluidics (Di Carlo et al., 2007; Di Carlo, 2009) and deterministic lateral displacement (Huang et al., 2004). Substantial future synergies will be achieved by combining the techniques, approaches, and insights of diverse biologists, biomechanics and fluid dynamics researchers, and engineers (including chemical, mechanical, biomedical, and filtration engineering). As biomimetics and bioinspired design continue to

expand, additional innovative solutions will be developed for particle separation with industrial and commercial applications. Nonlinear dynamics are a promising focus of research for microfluidics at moderate Re ($1 < Re < \sim 100$, Stoecklein and Di Carlo, 2019; Xia et al., 2021; Battat et al., 2022), and biological systems are inherently nonlinear. For example, nonlinearities arising from secondary flows (e.g., curved channels, oscillatory flow; Zhao et al., 2020) and the active and passive movement of oral cavity structures (BAs, GRs, and associated protrusions) during fish SF have the potential for nonintuitive effects on particle separation.

The novel particle separation mechanisms proposed recently in SF fishes are distinct from mechanisms described in SF invertebrates. This could be related to fundamental differences between SF fishes and most SF invertebrates, including (1) the oral cavity of SF fishes forms an enclosed porous channel or pipe, (2) all SF fishes are active suspension feeders with control over pore size, pressure, and flow velocity, and (3) the filter elements, pore sizes, and flow speeds can be larger in SF fishes, resulting in higher Re. All recently proposed particle separation mechanisms in SF fishes (inertial lift and shear-induced migration, reduction of effective gap size by vortices, cross-step filtration, vortical flow along outer faces of gill raker plates, ricochet filtration, lateral displacement) require crossflow in a channel or pipe, usually involving the generation of vortical flow. Studies of convergence/divergence in form and function of SF fishes and other SF vertebrates (e.g., tadpoles, flamingos and anatine ducks, balaenid and balaenopterid whales; Sanderson and Wassersug, 1993), as well as invertebrate taxa in which the filter elements operate in enclosed body cavities or tubes (e.g., Cephalochordata, Tunicata, Bivalvia, Brachiopoda; Hamann and Blanke, 2022) are also promising future directions.

Author contributions

SS: Conceptualization, Visualization, Writing – original draft, Writing – review & editing, Formal Analysis.

Funding

The author(s) declare that financial support was received for the research, authorship, and/or publication of this article. Supported by a research leave from William & Mary to SS, and by an international travel grant from the Reves Center for International Studies at William & Mary.

Acknowledgments

With gratitude and admiration for my graduate and post-doctoral mentors: Karel Liem, Richard Wassersug, Angela Cheer, and Joseph J. Cech, Jr., and appreciation for my collaborators. Special thanks to Mason Dean and Venkata A. Surapaneni for their expertise in initiating and organizing the Filters in Biology + Biomimetics conference, Berlin, May 2023.

Conflict of interest

SS is the inventor on US Patent No. 9,480,951; William & Mary, assignee. "Mass transfer device and system generating vortices for particle suspension, concentration, and transport", issued November 1, 2016.

Publisher's note

References

Adelmann, B., Schwiddessen, T., Götzendorfer, B., and Hellmann, R. (2022). Evaluation of SLS 3D-printed filter structures based on bionic manta structures. *Materials* 15, 8454. doi: 10.3390/ma15238454

Annis, E. R., Houde, E. D., Harding, L. W. Jr., Mallonee, M. E., and Wilberg, M. J. (2011). Calibration of a bioenergetics model linking primary production to Atlantic menhaden *Brevoortia tyrannus* growth in Chesapeake Bay. *Mar. Ecol. Prog. Ser.* 437, 253–267. doi: 10.3354/meps09254

Authimoolam, S. P., and Dziubla, T. D. (2016). Biopolymeric mucin and synthetic polymer analogs: Their structure, function, and role in biomedical applications. *Polymers* 8, 71. doi: 10.3390/polym8030071

Bansil, R., and Turner, B. S. (2018). The biology of mucus: Composition, synthesis and organization. *Adv. Drug Deliv. Rev.* 124, 3–15. doi: 10.1016/j.addr.2017.09.023

Battat, S., Weitz, D. A., and Whitesides, G. M. (2022). Nonlinear phenomena in microfluidics. *Chem. Rev.* 122, 6921–6937. doi: 10.1021/acs.chemrev.1c00985

Bayer, I. S. (2022). Recent advances in mucoadhesive interface materials, mucoadhesion characterization, and Technologies. *Adv. Mater. Interfaces* 9, 2200211. doi: 10.1002/admi.202200211

Bej, R., and Haag, R. (2022). Mucus-inspired dynamic hydrogels: Synthesis and future perspectives. *J. Am. Chem. Soc* 144, 20137–20152. doi: 10.1021/jacs.1c13547

Belfort, G., Davis, R. H., and Zydney, A. L. (1994). The behavior of suspensions and macromolecular solutions in crossflow microfiltration. *J. Membr. Sci.* 96, 1–58. doi: 10.1016/0376-7388(94)00119-7

Beveridge, M. C. M., Briggs, M. R. P., Northcott, M. E., and Ross, L. G. (1988). The occurrence, structure, and development of microbranchiospines among the tilapias (Cichlidae: Tilapiini). *Can. J. Zool.* 66, 2564–2572. doi: 10.1139/z88-377

Bianciardi, A., and Cascini, G. (2022). A bio-inspired approach for boosting innovation in the separation technology sector. *Proc. IMechE Part C: J. Mech. Eng. Sci.* 236, 4533–4550. doi: 10.1177/09544062211052128

Bouhid de Aguiar, I., and Schroën, K. (2020). Microfluidics used as a tool to understand and optimize membrane filtration processes. *Membranes* 10, 316. doi: 10.3390/membranes10110316

Brainerd, E. L. (2001). Caught in the crossflow. *Nature* 412, 387–388. doi: 10.1038/35086666

Brodnicke, O. B., Hansen, C. E., Huie, J. M., Brandl, S. J., and Worsaae, K. (2022). Functional impact and trophic morphology of small, sand-sifting fishes on coral reefs. *Funct. Ecol.* 36, 1936–1948. doi: 10.1111/1365-2435.14087

Brooks, H., Haines, G. E., Lin, M. C., and Sanderson, S. L. (2018). Physical modeling of vortical cross-step flow in the American paddlefish, *Polyodon spathula*. *PloS One* 13, e0193874. doi: 10.1371/journal.pone.0193874

Bulusu, K. V., Racan, S., and Plesniak, M. W. (2020). Macro-rheology characterization of gill raker mucus in the silver carp, *Hypophthalmichthys molitrix*. *J. Vis. Exp.* 161, e61379. doi: 10.3791/61379

Burns, C. A., Veldman, T. G., Serkowski, J., Daniel, R. C., Yu, X. Y., Minette, M. J., et al. (2021). Mesofluidic separation versus dead-end filtration. *Sep. Purif. Technol.* 254, 117256. doi: 10.1016/j.seppur.2020.117256

Callan, W. T., and Sanderson, S. L. (2003). Feeding mechanisms in carp: Crossflow filtration, palatal protrusions and flow reversals. *J. Exp. Biol.* 206, 883–892. doi: 10.1242/jeb.00195

Camp, A. L., Roberts, T. J., and Brainerd, E. L. (2015). Swimming muscles power suction feeding in largemouth bass. *Proc. Natl. Acad. Sci. U.S.A.* 112, 8690–8695. doi: 10.1073/pnas.1508055112

Cerullo, A. R., Lai, T. Y., Allam, B., Baer, A., Barnes, W. J. P., Barrientos, Z., et al. (2020). Comparative animal mucomics: Inspiration for functional materials from ubiquitous and understudied biopolymers. *ACS Biomater. Sci. Eng.* 6, 5377–5398. doi: 10.1021/acsbiomaterials.0c00713

Cheer, A., Cheung, S., Hung, T.-C., Piedrahita, R. H., and Sanderson, S. L. (2012). Computational fluid dynamics of fish gill rakers during crossflow filtration. *Bull. Math. Biol.* 74, 981–1000. doi: 10.1007/s11538-011-9709-6

Cheer, A. Y., Cheung, S., and Sanderson, S. L. (2006). "Computational fluid dynamics of crossflow filtration in suspension-feeding fishes," in *Computational Fluid Dynamics 2004*. Eds. C. Groth and D. W. Zingg (Springer, Berlin), 301–306. doi: 10.1007/3-540-31801-1_4

Cheer, A. Y., Ogami, Y., and Sanderson, S. L. (2001). Computational fluid dynamics in the oral cavity of ram suspension-feeding fishes. *J. Theor. Biol.* 210, 463–474. doi: 10.1006/jtbi.2001.2325

Chen, L., Asai, K., Nonomura, T., Xi, G., and Liu, T. (2018). A review of backward-facing step (BFS) flow mechanisms, heat transfer, and control. *Therm. Sci. Eng. Prog.* 6, 194–216. doi: 10.1016/j.tsep.2018.04.004

Chew, J. W., Kilduff, J., and Belfort, G. (2020). The behavior of suspensions and macromolecular solutions in crossflow microfiltration: An update. *J. Membr. Sci.* 601, 117865. doi: 10.1016/j.memsci.2020.117865

Ciechomski, J. (1967). Investigations of food and feeding habits of larvae and juveniles of the Argentine anchovy *Engraulis anchoita*. *Calif. Coop. Ocean. Fish. Investig. Rep.* 11, 72–81.

Clark, A. S., and San-Miguel, A. (2021). A bioinspired, passive microfluidic lobe filtration system. *Lab. Chip* 21, 3762. doi: 10.1039/D1LC00449B

Cohen, K. E., Ackles, A. L., and Hernandez, L. P. (2022). The role of heterotopy and heterochrony during morphological diversification of otocephalan epibranchial organs. *Evol. Dev.* 24, 79–91. doi: 10.1111/ede.12401

Cohen, K. E., George, A. E., Chapman, D. C., Chick, J. H., and Hernandez, L. P. (2020). Developmental ecomorphology of the epibranchial organ of the silver carp, *Hypophthalmichthys molitrix*. *J. Fish Biol.* 97, 527–536. doi: 10.1111/jfb.14409

Cohen, K. E., and Hernandez, L. P. (2018). Making a master filterer: Ontogeny of specialized filtering plates in silver carp (*Hypophthalmichthys molitrix*). *J. Morphol.* 2018, 1–11. doi: 10.1002/jmor.20821

Cohen, K. E., Hernandez, L. P., Crawford, C. H., and Flammang, B. E. (2018). Channeling vorticity: Modeling the filter-feeding mechanism in silver carp using μCT and 3D PIV. *J. Exp. Biol.* 221, jeb183350. doi: 10.1242/jeb.183350

Collard, F., Gilbert, B., Eppe, G., Roos, L., Compère, P., Das, K., et al. (2017). Morphology of the filtration apparatus of three planktivorous fishes and relation with ingested anthropogenic particles. *Mar. pollut. Bull.* 116, 182–191. doi: 10.1016/j.marpolbul.2016.12.067

Conley, K. R., Ben-Tal, A., Jacobi, Y., Yahel, G., and Sutherland, K. R. (2018a). Not-so-simple sieving by ascidians: re-examining particle capture at the mesh and organismal scales. *Mar. Biol.* 165, 45. doi: 10.1007/s00227-018-3300-8

Conley, K. R., Lombard, F., and Sutherland, K. R. (2018b). Mammoth grazers on the ocean's minuteness: A review of selective feeding using mucous meshes. *Proc. R. Soc B* 285, 20180056. doi: 10.1098/rspb.2018.0056

Cooper, R. L., Nicklin, E. F., Rasch, L. J., and Fraser, D. J. (2023). Teeth outside the mouth: The evolution and development of shark denticles. *Evol. Dev.* 25, 54–72. doi: 10.1111/ede.12427

Couturier, L. I. E., Rohner, C. A., Richardson, A. J., Marshall, A. D., Jaine, F. R. A., Bennett, M. B., et al. (2013a). Stable isotope and signature fatty acid analyses suggest reef manta rays feed on demersal zooplankton. *PloS One* 8, e77152. doi: 10.1371/journal.pone.0077152

Couturier, L. I. E., Rohner, C. A., Richardson, A. J., Pierce, S. J., Marshall, A. D., Jaine, F. R. A., et al. (2013b). Unusually high levels of n-6 polyunsaturated fatty acids in whale sharks and reef manta rays. *Lipids* 48, 1029–1034. doi: 10.1007/s11745-013-3829-8

Day, S. W., Higham, T. E., Holzman, R., and Van Wassenbergh, S. (2015). Morphology, kinematics, and dynamics: The mechanics of suction feeding in fishes. *Integr. Comp. Biol.* 55, 21–35. doi: 10.1093/icb/icv032

De Sales-Ribeiro, C., Brito-Casillas, Y., Fernandez, A., and Caballero, M. J. (2020). An end to the controversy over the microscopic detection and effects of pristine microplastics in fish organs. *Sci. Rep.* 10, 12434. doi: 10.1038/s41598-020-69062-3

Di Carlo, D. (2009). Inertial microfluidics. *Lab. Chip* 9, 3038–3046. doi: 10.1039/b912547g

Di Carlo, D., Edd, J. F., Humphry, K. J., Stone, H. A., and Toner, M. (2009). Particle segregation and dynamics in confined flows. *Phys. Rev. Lett.* 102, 94503. doi: 10.1103/PhysRevLett.102.094503

Di Carlo, D., Irimia, D., Tompkins, R. G., and Toner, M. (2007). Continuous inertial focusing, ordering, and separation of particles in microchannels. *Proc. Natl. Acad. Sci. U.S.A.* 104, 18892–18897. doi: 10.1073/pnas.0704958104

Dijkshoorn, J. P., de Valença, J. C., Wagterveld, R. M., Boom, R. M., and Schutyser, M. A. (2018). Visualizing the hydrodynamics in sieve-based lateral displacement systems. *Sci. Rep.* 8, 12861. doi: 10.1038/s41598-018-31104-2

Dijkshoorn, J. P., Schutyser, M. A. I., Wagterveld, R. M., Schroën, C. G. P. H., and Boom, R. M. (2017). A comparison of microfiltration and inertia-based microfluidics for large scale suspension separation. *Sep. Purif. Technol.* 173, 86–92. doi: 10.1016/j.seppur.2016.09.018

Dincau, B., Tang, C., Dressaire, E., and Sauret, A. (2022). Clog mitigation in a microfluidic array *via* pulsatile flows. *Soft Matter* 18, 1767–1778. doi: 10.1039/D2SM00013J

Di Vaira, N. J., Laniewski-Wollk, L., Johnson, R. L. Jr., Aminossadati, S. M., and Leonardi, C. R. (2022). Influence of particle polydispersity on bulk migration and size segregation in channel flows. *J. Fluid Mech.* 939, A30. doi: 10.1017/jfm.2022.166

Divi, R. V., Strother, J. A., and Paig-Tran, E. W. M. (2018). Manta rays feed using ricochet separation, a novel nonclogging filtration mechanism. *Sci. Adv.* 4, eaat9533. doi: 10.1126/sciadv.aat9533

Dou, Y., Tian, D., Sun, Z., Liu, Q., Zhang, N., Kim, J. H., et al. (2017). Fish gill inspired crossflow for efficient and continuous collection of spilled oil. *ACS Nano* 11, 2477–2485. doi: 10.1021/acsnano.6b07918

Drenner, R. W., Hambright, K. D., Vinyard, G. L., and Gophen, M. (1987). Particle ingestion by *Tilapia galilaea* is not affected by removal of gill rakers and microbranchiospines. *Trans. Am. Fish. Soc* 116, 272–276. doi: 10.1577/1548-8659(1987)116<272:PIBTGI>2.0.CO;2

Drenner, R. W., Mummert, J. R., deNoyelles, F. Jr., and Kettle, D. (1984). Selective particle ingestion by a filter-feeding fish and its impact on phytoplankton community structure. *Limnol. Oceanogr.* 29, 941–948. doi: 10.4319/lo.1984.29.5.0941

Drijer, I., and Schroën, K. (2018). Modelling shear induced diffusion based particle segregation: A basis for novel separation technology. *Appl. Sci.* 8, 108. doi: 10.3390/app8061008

Edwards, K. M., Rice, G. W., and Sanderson, S. L. (2017). Separating oil from water: Suspension-feeding goldfish ingest liquid vegetable oil. *Can. J. Fish. Aquat. Sci.* 74, 524–532. doi: 10.1139/cjfas-2016-0197

Espinosa-Gayosso, A., Ghisalberti, M., Shimeta, J., and Ivey, G. N. (2021). On predicting particle capture rates in aquatic ecosystems. *PloS One* 16, e0261400. doi: 10.1371/journal.pone.0261400

Estrada, J. A., Lutcavage, M., and Thorrold, S. R. (2005). Diet and trophic position of Atlantic bluefin tuna (*Thunnus thynnus*) inferred from stable carbon and nitrogen isotope analysis. *Mar. Biol.* 147, 37–45. doi: 10.1007/s00227-004-1541-1

FAO (2021). *FAO yearbook. Fishery and Aquaculture Statistics 2019* (Rome: Food and Agriculture Organization of the United Nations).

Friedland, K. D. (1985). Functional morphology of the branchial basket structures associated with feeding in the Atlantic menhaden, *Brevoortia tyrannus* (Pisces: Clupeidae). *Copeia* 1985, 1018–1027. doi: 10.2307/1445257

Friedland, K. D., Ahrenholz, D. W., Smith, J. W., Manning, M., and Ryan, J. (2006). Sieving functional morphology of the gill raker feeding apparatus of Atlantic menhaden. *J. Exp. Zool. A Comp. Exp. Biol.* 305, 974–985. doi: 10.1002/(ISSN)1552-499X

Friedland, K. D., Haas, L. W., and Merriner, J. V. (1984). Filtering rates of the juvenile Atlantic menhaden *Brevoortia tyrannus* (Pisces: Clupeidae), with consideration of the effects of detritus and swimming speed. *Mar. Biol.* 84, 109–117. doi: 10.1007/BF00392994

Gerking, S. D. (1994). *Feeding Ecology of Fish* (San Diego: Academic Press).

Gibson, R. N. (1988). Development, morphometry and particle retention capability of the gill rakers in the herring, *Clupea harengus* L. *J. Fish Biol.* 32, 949–962. doi: 10.1111/j.1095-8649.1988.tb05438.x

Goel, G., Hélix-Nielsen, C., Upadhyaya, H. M., and Goel, S. (2021). A bibliometric study on biomimetic and bioinspired membranes for water filtration. *NPJ Clean Water* 4, 41. doi: 10.1038/s41545-021-00131-4

Goldbogen, J. A., Pyenson, N. D., and Shadwick, R. E. (2007). Big gulps require high drag for fin whale lunge feeding. *Mar. Ecol. Prog. Ser.* 349, 289–301. doi: 10.3354/meps07066

Goodrich, J. S., Sanderson, S. L., Batjakas, I. E., and Kaufman, L. S. (2000). Branchial arches of suspension-feeding *Oreochromis esculentus*: Sieve or sticky filter? *J. Fish Biol.* 56, 858–875. doi: 10.1006/jfbi.1999.1205

Haines, G. E., and Sanderson, S. L. (2017). Integration of swimming kinematics and ram suspension feeding in a model American paddlefish, *Polyodon spathula*. *J. Exp. Biol.* 220, 4535–4547. doi: 10.1242/jeb.166835

Hamann, L., and Blanke, A. (2022). Suspension feeders: Diversity, principles of particle separation and biomimetic potential. *J. R. Soc Interface* 19, 20210741. doi: 10.1098/rsif.2021.0741

Hamann, L., Schreiber, K., Hagenmeyer, J., Eduardo, S., Spanke, T., and Blanke, A. (2023). Diversity of filter feeding and variations in cross-flow filtration of five ram-feeding fish species. *Front. Mar. Sci.* 10. doi: 10.3389/fmars.2023.1253083

Hansen, A., Ghosal, R., Caprio, J., Claus, A. W., and Sorensen, P, W. (2014). Anatomical and physiological studies of bigheaded carps demonstrate that the epibranchial organ functions as a pharyngeal taste organ. *J. Exp. Biol.* 217, 3945–3954. doi: 10.1242/jeb.107870

Harrison, I. J., and Howes, G. J. (1991). The pharyngobranchial organ of mugilid fishes: Its structure, variability, ontogeny, possible function, and taxonomic utility. *Bull. Br. Museum Natural History Zoology* 57, 111–132.

Hentschel, B. T., and Shimeta, J. (2019). "Suspension feeders," in *Encyclopedia of Ecology*, *2nd edition*, vol. 3 . Eds. S. E. Jørgensen and B. D. Fath (Academic Press, Oxford), 624–629. doi: 10.1016/B978-0-12-409548-9.11133-9

Hochstetter, A., Vernekar, R., Austin, R. H., Becker, H., Beech, J. P., Fedosov, D. A., et al. (2020). Deterministic lateral displacement: Challenges and perspectives. *ACS Nano* 14, 10784–10795. doi: 10.1021/acsnano.0c05186

Holley, L. L., Heidman, M. K., Chambers, R. M., and Sanderson, S. L. (2015). Mucous contribution to gut nutrient content in American gizzard shad *Dorosoma cepedianum*. *J. Fish Biol.* 86, 1457–1470. doi: 10.1111/jfb.12656

Hong, K.-B., Kim, D.-W., Kwark, J., Nam, J.-S., and Ryou, H.-S. (2021). Numerical study on the effect of the pipe groove height and pitch on the flow characteristics of corrugated pipe. *Energies* 14, 2614. doi: 10.3390/en14092614

Hoogenboezem, W. (2000). On the feeding biology of bream (*Abramis brama*). *Neth. J. Zool.* 50, 225–232. doi: 10.1163/156854200505964

Hoogenboezem, W., and van den Boogaart, J. G. M. (1993). Importance of mucus in filter-feeding of bream (*Abramis brama*). *Can. J. Fish. Aquat. Sci.* 50, 472–479. doi: 10.1139/f93-055

Hoogenboezem, W., van den Boogaart, J. G. M., Sibbing, F. A., Lammens, E. H. R. R., Terlouw, A., and Osse, J. W. M. (1991). A new model of particle retention and branchial sieve adjustment in filter-feeding bream (*Abramis brama*, Cyprinidae). *Can. J. Fish. Aquat. Sci.* 48, 7–18. doi: 10.1139/f91-002

Huang, L. R., Cox, E. C., Austin, R. H., and Sturm, J. C. (2004). Continuous particle separation through deterministic lateral displacement. *Science* 304, 5673. doi: 10.1126/science.1094567

Hung, T. C., and Piedrahita, R. H. (2014). Experimental validation of a novel bio-inspired particle separator. *Aquac. Eng.* 58, 11–19. doi: 10.1016/j.aquaeng.2013.09.005

Hung, T. C., Piedrahita, R. H., and Cheer, A. (2012). Bio-inspired particle separator design based on the food retention mechanism by suspension-feeding fish. *Bioinspir. Biomim.* 7, 46003. doi: 10.1088/1748-3182/7/4/046003

Ibrahim, A. N. A. F., Castilho Noll, M. S. M., and Valenti, W. C. (2015). Zooplankton capturing by Nile tilapia, *Oreochromis niloticus* (Teleostei: Cichlidae) throughout post-larval development. *Zoologia* 32, 469–475. doi: 10.1590/s1984-46702015000600006

Idris, I., Moloney, C. L., and van der Lingen, C. D. (2016). Spatial variability in branchial basket meristics and morphology of southern African sardine *Sardinops sagax*. *Afr. J. Mar. Sci.* 38, 351–362. doi: 10.2989/1814232X.2016.1204942

Imms, A. D. (1904). Notes on the gill-rakers of the spoonbill sturgeon, *Polyodon spathula*. *Proc. Zool. Soc Lond.* 2, 22–35. doi: 10.1111/j.1469-7998.1904.tb08311.x

Irschick, D. J., Christiansen, F., Hammerschlag, N., Martin, J., Madsen, P. T., Wyneken, J., et al. (2022). 3D visualization processes for recreating and studying organismal form. *iScience* 25, 104867. doi: 10.1016/j.isci.2022.104867

Jørgensen, C. B. (1966). *Biology of Suspension Feeding* (New York: Pergamon).

Kenaley, C. P., and Lauder, G. V. (2016). A biorobotic model of the suction-feeding system in largemouth bass: The roles of motor program speed and hyoid kinematics. *J. Exp. Biol.* 219, 2048–2059. doi: 10.1242/jeb.132514

Kirchhoff, H. (1958). Funktionell-anatomische untersuchung des visceralapparates von *Clupea harengus* L. *Zoologisches Jahrbücher Abteilung für Anatomie und Ontogenie der Tiere* 76, 461–540.

Kolar, C. S., Chapman, D. C., Courtenay, W. R.Jr., Housel, C. M., Williams, J. D., and Jennings, D. P. (2007). *Bigheaded carps: A biological synopsis and environmental risk assessment* (Bethesda, Maryland: American Fisheries Society, Special Publication 33).

Kumar, G. P., and Das, A. K. (2022). Hybrid microfluidic design for separation of neutrally-buoyant and non-buoyant particles. *Chem. Eng. Process.: Process Intensif.* 180, 108721. doi: 10.1016/j.cep.2021.108721

LaBarbera, M. (1984). Feeding currents and particle capture mechanisms in suspension feeding animals. *Amer. Zool.* 24, 71–84. doi: 10.1093/icb/24.1.71

Lang, T., Klasson, S., Larsson, E., Johansson, M. E. V., Hansson, G. C., and Samuelsson, T. (2016) Searching the evolutionary origin of epithelial mucus protein components — Mucins and FCGBP. *Mol. Biol. Evol.* 33, 1921–1936. doi: 10.1093/molbev/msw066

Langeland, A., and Nøst, T. (1995). Gill raker structure and selective predation on zooplankton by particulate feeding fish. *J. Fish Biol.* 47, 719–732. doi: 10.1111/j.1095-8649.1995.tb01937.x

Larson, E. T., and Shanks, A. L. (1996). Consumption of marine snow by two species of juvenile mullet and its contribution to their growth. *Mar. Ecol. Prog. Ser.* 130, 19–28. doi: 10.3354/meps130019

Lazarro, X. (1987). A review of planktivorous fishes: Their evolution, feeding behaviours, selectivities, and impact. *Hydrobiologia* 146, 97–167. doi: 10.1007/BF00008764

Lee, S., Kim, H., and Yang, S. (2023). Microfluidic label-free hydrodynamic separation of blood cells: Recent developments and future perspectives. *Adv. Mater. Technol.* 8, 2201425. doi: 10.1002/admt.202201425

Letendre, F., and Cameron, C. B. (2022). The capture of crude oil droplets by filter feeders at high and low Reynolds numbers. *J. Exp. Biol.* 225, jeb243819. doi: 10.1242/jeb.243819

Letendre, F., Mehrabian, S., Etienne, S., and Cameron, C. B. (2020). The interactions of oil droplets with filter feeders: A fluid mechanics approach. *Mar. Environ. Res.* 161, 105059. doi: 10.1016/j.marenvres.2020.105059

Lewis, V. P., and Peters, D. S. (1994). Diet of juvenile and adult Atlantic menhaden in estuarine and coastal habitats. *Trans. Am. Fish. Soc* 123, 803–810. doi: 10.1577/1548-8659(1994)123<0803:DOJAAA>2.3.CO;2

Li, Z., Tan, C. M., Tio, W., Ang, J., and Sun, D. D. (2018). Manta ray gill inspired radially distributed nanofibrous membrane for efficient and continuous oil-water separation. *Environ. Sci.:Nano* 5, 1466. doi: 10.1039/C8EN00258D

Lürling, M., and Mucci, M. (2020). Mitigating eutrophication nuisance: in-lake measures are becoming inevitable in eutrophic waters in the Netherlands. *Hydrobiologia* 847, 4447–4467. doi: 10.1007/s10750-020-04297-9

Lysenko, D. A., Donskov, M., and Ertesvåg, I. S. (2023). Large-eddy simulations of the flow past a bluff-body with active flow control based on trapped vortex cells at Re = 50000. *Ocean Eng.* 280, 114496. doi: 10.1016/j.oceaneng.2023.114496

Magnuson, J. J., and Heitz, J. G. (1971). Gill raker apparatus and food selectivity among mackerels, tunas, and dolphins. *Fish. Bull.* 69, 361–370.

Martel, J. M., and Toner, M. (2014). Inertial focusing in microfluidics. *Annu. Rev. Biomed. Eng.* 16, 371–396. doi: 10.1146/annurev-bioeng-121813-120704

Masselter, T., Schaumann, U., Kampowski, T., Ulrich, K., Thielen, M., Bold, G., et al. (2023). Improvement of a microfiber filter for domestic washing machines. *Bioinspir. Biomim.* 18, 016017. doi: 10.1088/1748-3190/acaba2

Matthews, L. H., and Parker, H. W. (1950). Notes on the anatomy and biology of the basking shark (*Cetorhinus maximus* [Gunner]). *Proc. Zool. Soc Lond.* 120, 535–576. doi: 10.1111/j.1096-3642.1950.tb00663.x

Meekan, M. G., Virtue, P., Marcus, L., Clements, K. D., Nichols, P. D., and Revill, A. T. (2022). The world's largest omnivore is a fish. *Ecology* 103, e3818. doi: 10.1002/ecy.3818

Misic, C., Capone, A., and Petrillo, M. (2022). Meteorological and climatic variability influences anthropogenic microparticle content in the stomach of the European anchovy *Engraulis encrasicolus*. *Hydrobiologia* 849, 589–602. doi: 10.1007/s10750-021-04727-2

Montazer, E., Yarmand, H., Salami, E., Muhamad, M. R., Kazi, S. N., and Badarudin, A. (2018). A brief review study of flow phenomena over a backward-facing step and its optimization. *Renew. Sust. Energ. Rev.* 82, 994–1005. doi: 10.1016/j.rser.2017.09.104

Mori, S., and Nakamura, T. (2022). Redeployment of odontode gene regulatory network underlies dermal denticle formation and evolution in suckermouth armored catfish. *Sci. Rep.* 12, 6172. doi: 10.1038/s41598-022-10222-y

Morris, C. C., and Deibel, D. (1993). Flow rate and particle concentration within the house of the pelagic tunicate *Oikopleura vanhoeffeni*. *Mar. Biol.* 115, 445–452. doi: 10.1007/BF00349843

Motta, P. J., Maslanka, M., Hueter, R. E., Davis, R. L., de la Parra, R., Mulvany, S. L., et al. (2010). Feeding anatomy, filter-feeding rate, and diet of whale sharks *Rhincodon typus* during surface ram filter feeding off the Yucatan Peninsula, Mexico. *Zoology* 113, 199–212. doi: 10.1016/j.zool.2009.12.001

Mummert, J. R., and Drenner, R. W. (1986). Effect of fish size on the filtering efficiency and selective particle ingestion of a filter-feeding clupeid. *Trans. Am. Fish. Soc* 115, 522–528. doi: 10.1577/1548-8659(1986)115<522:EOFSOT>2.0.CO;2

Nelson, G. T. (1967a). Gill arches of teleostean fishes of the family Clupeidae. *Copeia* 1967, 389–399. doi: 10.2307/1442129

Northcott, M. E., and Beveridge, M. C. M. (1988). The development and structure of pharyngeal apparatus associated with filter feeding in tilapias (*Oreochromis niloticus*). *J. Zool. Lond.* 215, 133–149. doi: 10.1111/j.1469-7998.1988.tb04889.x

Nunes, S. A., Magalhães, H. L. F., Gomez, R. S., Vilela, A. F., Figueiredo, M. J., Santos, R. S., et al. (2021). Oily water separation process using hydrocyclone of porous membrane wall: A numerical investigation. *Membranes* 11, 79. doi: 10.3390/membranes11020079

Olsen, A. M., Hernandez, L. P., and Brainerd, E. L. (2020). Multiple degrees of freedom in the fish skull and their relation to hydraulic transport in channel catfish. *Integr. Org. Biol.* 2, obaa031. doi: 10.1093/iob/obaa031

Paig-Tran, E. W. M., Bizzarro, J. J., Strother, J. A., and Summers, A. P. (2011). Bottles as models: Predicting the effects of varying swimming speed and morphology on size selectivity and filtering efficiency in fishes. *J. Exp. Biol.* 214, 1643–1654. doi: 10.1242/jeb.048702

Paig-Tran, E. W. M., Kleinteich, T., and Summers, A. P. (2013). The filter pads and filtration mechanisms of the devil rays: Variation at macro and microscopic scales. *J. Morphol.* 274, 1026–1043. doi: 10.1002/jmor.20160

Paig-Tran, E. W. M., and Summers, A. P. (2014). Comparison of the structure and composition of the branchial filters in suspension feeding elasmobranchs. *Anat. Rec.* 297, 701–715. doi: 10.1002/ar.22850

Paskin, M., Baum, D., Dean, M. N., and von Tycowicz, C. (2022). "A Kendall shape space approach to 3D shape estimation from 2D landmarks," in Proceedings of the

European Conference on Computer Vision 2022: 17th European Conference, *Tel Aviv, ISRAEL, October 23-27*. Eds. S. Avidan, G. Brostow, M. Cissé, G. M. Farinella and T. Hassner (Springer-Verlag, Berlin). doi: 10.1007/978-3-031-20086-1_21

Pease, L. F., Philips, N. R., Serkowski, J., Veldman, T. G., Minette, M. J., and Burns, C. A. (2022). Industrial scale mesofluidic particle separation. *Chem. Eng. Proc.: Proc. Intensif.* 173, 108795. doi: 10.1016/j.cep.2022.108795

Potvin, J., Goldbogen, J. A., and Shadwick, R. E. (2009). Passive versus active engulfment: Verdict from trajectory simulations of lunge-feeding fin whales *Balaenoptera physalus*. *J. R. Soc Interface* 6, 1005–1025. doi: 10.1098/rsif.2008.0492

Presti, P., Johnson, G. D., and Datovo, A. (2020). Facial and gill musculature of polynemid fishes, with notes on their possible relationships with sciaenids (Percomorphacea: Perciformes). *J. Morphol.* 281, 662–675. doi: 10.1002/jmor.21134

Provini, P., Brunet, A., Filippo, A., and Van Wassenbergh, S. (2022). *In vivo* intraoral waterflow quantification. *eLife* 11, e73621. doi: 10.7554/eLife.73621

Riisgård, H. U., and Larsen, P. S. (2010). Particle capture mechanisms in suspension-feeding invertebrates. *Mar. Ecol. Prog. Ser.* 418, 255–293. doi: 10.3354/meps08755

Ron, E. Z., and Rosenberg, E. (2001). Natural roles of biosurfactants. *Environ. Microbiol.* 3, 229–236. doi: 10.1046/j.1462-2920.2001.00190.x

Rosen, R. A., and Hales, D. C. (1981). Feeding of paddlefish, Polyodon spathula. *Copeia* 1981, 441–455. doi: 10.2307/1444235

Ross, S. T. (2013). *Ecology of North American Freshwater Fishes* (Berkeley: University of California Press).

Rubenstein, D. I., and Koehl, M. A. R. (1977). The mechanisms of filter feeding: Some theoretical considerations. *Am. Nat.* 111, 981–994. doi: 10.1086/283227

Rykaczewski, R. R. (2009). "Influence of oceanographic variability on the planktonic prey and growth of sardine and anchovy in the California Current Ecosystem," in *Scripps Institution of Oceanography Technical Report* (Scripps Institution of Oceanography, UC San Diego). Available at: http://escholarship.org/uc/item/307453xf.

Salafi, T., Zhang, Y., and Zhang, Y. (2019). A review on deterministic lateral displacement for particle separation and detection. *Nano-Micro Lett.* 11, 77. doi: 10.1007/s40820-019-0308-7

Salman, S., Abu Talib, A. R., Saadon, S., and Hameed Sultan, M. T. (2020). Hybrid nanofluid flow and heat transfer over backward and forward steps: A review. *Powder Technol.* 363, 448–472. doi: 10.1016/j.powtec.2019.12.038

Sanderson, S. L., Cech, J. J.Jr., and Cheer, A. Y. (1994). Paddlefish buccal flow velocity during ram suspension feeding and ram ventilation. *J. Exp. Biol.* 186, 145–156. doi: 10.1242/jeb.186.1.145

Sanderson, S. L., Cech, J. J. Jr., and Patterson, M. R. (1991). Fluid dynamics in suspension-feeding blackfish. *Science* 251, 1346–1348. doi: 10.1126/science.251.4999.1346

Sanderson, S. L., Cheer, A. Y., Goodrich, J. S., Graziano, J. D., and Callan, W. T. (2001). Crossflow filtration in suspension-feeding fishes. *Nature* 412, 439–441. doi: 10.1038/35086574

Sanderson, S. L., Chesnutt, C. R., and Lobel, P. S. (1996a). Evidence for ram suspension feeding by the piscivore, *Seriola dumerili* (Carangidae). *Env. Biol. Fish.* 46, 365–373. doi: 10.1007/BF00005014

Sanderson, S. L., Mort, M. E., and Cech, J. J. Jr. (1998). Particle retention by non-suspension-feeding cyprinid fishes. *Can. J. Fish. Aquat. Sci.* 55, 861–868. doi: 10.1139/f97-292

Sanderson, S. L., Roberts, E., Lineburg, J., and Brooks, H. (2016). Fish mouths as engineering structures for vortical cross-step filtration. *Nat. Commun.* 7, 11092. doi: 10.1038/ncomms11092

Sanderson, S. L., Stebar, M. C., Ackermann, K. L., Jones, S. H., Batjakas, I. E., and Kaufman, L. (1996b). Mucus entrapment of particles by a suspension-feeding tilapia (Pisces: Cichlidae). *J. Exp. Biol.* 199, 1743–1756. doi: 10.1242/jeb.199.8.1743

Sanderson, S. L., and Wassersug, R. (1990). Suspension-feeding vertebrates. *Sci. Am.* 262, 96–102. doi: 10.1038/scientificamerican0390-96

Sanderson, S. L., and Wassersug, R. (1993). "Convergent and alternative designs for vertebrate suspension feeding," in *The Skull, Volume 3: Functional and Evolutionary Mechanisms*. Eds. J. Hanken and B. K. Hall (The University of Chicago Press, Chicago), 37–112.

Savoca, M. S., McInturf, A. G., and Hazen, E. L. (2020). Plastic ingestion by marine fish is widespread and increasing. *Glob. Change Biol.* 27, 2188–2189. doi: 10.1111/gcb.15533

Sazima, I. (1998). Field evidence for suspension feeding in *Pseudocaranx dentex*, with comments on ram filtering in other jacks (Carangidae). *Env. Biol. Fish.* 53, 225–229. doi: 10.1023/A:1007492803796

Schroeder, A., Marshall, L., Trease, B., Becker, A., and Sanderson, S. L. (2019). Development of helical, fish-inspired cross-step filter for collecting harmful algae. *Bioinspir. Biomim.* 14, 056008. doi: 10.1088/1748-3190/ab2d13

Schroën, K., van Dinther, A., and Stockmann, R. (2017). Particle migration in laminar shear fields: A new basis for large scale separation technology? *Sep. Purif. Technol.* 174, 372–388. doi: 10.1016/j.seppur.2016.10.057

Seghers, B. H. (1975). Role of gill rakers in size-selective predation by lake whitefish, *Coregonus clupeaformis* (Mitchill). *Verh. Internat. Verein. Limnol.* 19, 2401–2405. doi: 10.1080/03680770.1974.11896323

Shephard, K. L. (1994). Functions for fish mucus. *Rev. Fish Biol. Fish.* 4, 401–429. doi: 10.1007/BF00042888

Shimeta, J., and Jumars, P. A. (1991). Physical mechanisms and rates of particle capture by suspension-feeders. *Oceanogr. Mar. Biol. Annu. Rev.* 29, 191–257.

Sibbing, F. A., and Nagelkerke, L. A. J. (2001). Resource partitioning by Lake Tana barbs predicted from fish morphometrics and prey characteristics. *Rev. Fish Biol. Fish.* 10, 393–437. doi: 10.1023/A:1012270422092

Sibbing, F. A., and Uribe, R. (1985). Regional specializations in the oro-pharyngeal wall and food processing in the carp (*Cyprinus carpio* L.). *Neth. J. Zool.* 35, 377–422. doi: 10.1163/002829685X00280

Smith, J. C., and Sanderson, S. L. (2007). Mucus function and crossflow filtration in a fish with gill rakers removed versus intact. *J. Exp. Biol.* 210, 2706–2713. doi: 10.1242/jeb.000703

Smith, J. C., and Sanderson, S. L. (2008). Intra-oral flow patterns and speeds in a suspension-feeding fish with gill rakers removed versus intact. *Biol. Bull.* 215, 309–318. doi: 10.2307/25470714

Smith, J. C., and Sanderson, S. L. (2013). Particle retention in suspension-feeding fish after removal of filtration structures. *Zoology* 116, 348–355. doi: 10.1016/j.zool.2013.08.008

Springer, V. G., and Johnson, G. D. (2004). Study of the dorsal gill-arch musculature of teleostome fishes, with special reference to the Actinopterygii. *Bull. Biol. Soc Wash.* 11, 1–260. doi: 10.5962/bhl.title.49077

Stel, H., Franco, A. T., Junqueira, S. L. M., Erthal, R. H., Mendes, R., Gonçalves, M. A. L., et al. (2012). Turbulent flow in d-type corrugated pipes: flow pattern and friction factor. *J. Fluids Eng.* 134, 121202. doi: 10.1115/1.4007899

Stoecklein, D., and Di Carlo, D. (2019). Nonlinear microfluidics. *Anal. Chem.* 91, 296–314. doi: 10.1021/acs.analchem.8b05042

Storm, T. J., Nolan, K. E., Roberts, E. M., and Sanderson, S. L. (2020). Oropharyngeal morphology related to filtration mechanisms in suspension-feeding American shad (Clupeidae). *J. Exp. Zool. A Ecol. Integr. Physiol.* 333, 493–510. doi: 10.1002/jez.2363

Su, R., Li, S., Wu, W., Song, C., Liu, G., and Yu, Y. (2021). Recent progress in electrospun nanofibrous membranes for oil/water separation. *Sep. Purif. Technol.* 256, 117790. doi: 10.1016/j.seppur.2020.117790

Surapaneni, V. A., Schindler, M., Ziege, R., de Faria, L. C., Wölfer, J., Bidan, C. M., et al. (2022). Groovy and gnarly: Surface wrinkles as a multifunctional motif for terrestrial and marine environments. *Integr. Comp. Biol.* 62, 749–761. doi: 10.1093/icb/icac079

Tang, H., Niu, J., Jin, H., Lin, S., and Cui, D. (2022). Geometric structure design of passive label-free microfluidic systems for biological micro-object separation. *Microsyst. Nanoeng.* 8, 62. doi: 10.1038/s41378-022-00386-y

Turner, J. T. (2015). Zooplankton fecal pellets, marine snow, phytodetritus and the ocean's biological pump. *Prog. Oceanogr.* 130, 205–248. doi: 10.1016/j.pocean.2014.08.005

van den Berg, C., van den Boogaart, J. G. M., Sibbing, F. A., and Osse, J. W. M. (1993). Zooplankton feeding in common bream (*Abramis brama*), white bream (*Blicca bjoerkna*) and roach (*Rutilus rutilus*): Experiments, models and energy intake. *Neth. J. Zool.* 44, 15–42. doi: 10.1163/156854294X00024

van den Berg, C., van den Boogaart, J. G. M., Sibbing, F. A., and Osse, J. W. M. (1994a). Implications of gill arch movements for filter-feeding: An X-ray cinematographical study of filter-feeding white bream (*Blicca bjoerkna*) and common bream (*Abramis brama*). *J. Exp. Biol.* 191, 257–282. doi: 10.1242/jeb.191.1.257

van den Berg, C., van Snik, G. J. M., van den Boogaart, J. G. M., and Sibbing, F. A. (1994b). Comparative microanatomy of the branchial sieve in three sympatric cyprinid species, related to filter-feeding. *J. Morphol.* 219, 73–87. doi: 10.1002/jmor.1052190109

Vandewalle, P., Parmentier, É., and Chardon, M. (2000). The branchial basket in teleost feeding. *Cybium* 24, 319–342.

van Dinther, A. M. C., Schroën, C. G. P. H., and Boom, R. M. (2013a). Particle migration leads to deposition-free fractionation. *J. Membr. Sci.* 440, 58–66. doi: 10.1016/j.memsci.2013.03.050

van Dinther, A. M. C., Schroën, C. G. P. H., Imhof, A., Vollebregt, H. M., and Boom, R. M. (2013b). Flow-induced particle migration in microchannels for improved microfiltration processes. *Microfluid. Nanofluid.* 15, 451–465. doi: 10.1007/s10404-013-1158-0

Van Wassenbergh, S., and Sanderson, S. L. (2023). Hydrodynamic analysis of bioinspired vortical cross-step filtration by computational modelling. *R. Soc Open Sci.* 10, 230315. doi: 10.1098/rsos.230315

Voskuhl, L., and Rahlff, J. (2022). Natural and oil surface slicks as microbial habitats in marine systems: A review. *Front. Mar. Sci.* 9. doi: 10.3389/fmars.2022.1020843

Wang, J. M., Jin, Q. Q., Zhang, Y. Y., Fang, H. C., and Xia, H. M. (2021). Reducing the membrane fouling in cross-flow filtration using a facile fluidic oscillator. *Sep. Purif. Technol.* 272, 118854. doi: 10.1016/j.seppur.2021.118854

Wegner, N. C. (2015). "Elasmobranch gill structure," in *Physiology of Elasmobranch Fishes: Structure and Interaction with Environment, Fish Physiology*, vol. 34A . Eds. R. E. Shadwick, A. P. Farrell and C. J. Brauner (London: Elsevier Science and Technology), 101–151. doi: 10.1016/B978-0-12-801289-5.00003-1

Weller, H. I., McMahan, C. D., and Westneat, M. W. (2017). Dirt-sifting devilfish: winnowing in the geophagine cichlid *Satanoperca daemon* and evolutionary implications. *Zoomorphology* 136, 45–59. doi: 10.1007/s00435-016-0335-6

Werth, A. J., and Potvin, J. (2016). Baleen hydrodynamics and morphology of cross-flow filtration in balaenid whale suspension feeding. *PloS One* 11, e0150106. doi: 10.1371/journal.pone.0150106

Winterbottom, R. (1974). A descriptive synonymy of the striated muscles of the Teleostei. *Proc. Acad. Nat. Sci. Philadelphia* 125, 225–317.

Witkop, E. M., Van Wassenbergh, S., Heideman, P. D., and Sanderson, S. L. (2023). Biomimetic models of fish gill rakers as lateral displacement arrays for particle separation. *Bioinspir. Biomim.* 18, 056009. doi: 10.1088/1748-3190/acea0e

Wright, D. I., O'Brien, W. J., and Luecke, C. (1983). A new estimate of zooplankton retention by gill rakers and its ecological significance. *Trans. Am. Fish. Soc* 112, 638–646. doi: 10.1577/1548-8659(1983)112<638:ANEOZR>2.0.CO;2

Xia, H. M., Wu, J. W., Zheng, J. J., Zhang, J., and Wang, Z. P. (2021). Nonlinear microfluidics: device physics, functions, and applications. *Lab. Chip* 21, 1241–1268. doi: 10.1039/D0LC01120G

Xiang, N., and Ni, Z. (2022). Inertial microfluidics: Current status, challenges, and future opportunities. *Lab. Chip* 22, 4792. doi: 10.1039/D2LC00722C

Xu, Z., Mao, X., Gu, Y., Chen, X., Kuang, W., Wang, R., et al. (2023). Analysis of hydrodynamic filtration performance in a cross-step filter for drip irrigation based on the CFD-DEM coupling method. *Biosyst. Eng.* 232, 114–128. doi: 10.1016/j.biosystemseng.2023.07.004

Yang, M., Hou, L., Wang, L., Liu, S., and Xu, J. (2022). Effect of oil properties on spilled oil recovery using a mechanism coupling surface vortices and cyclone separation. *Ocean Eng.* 263, 112383. doi: 10.1016/j.oceaneng.2022.112383

Zhang, K., Ma, C., Zhang, J., Zhang, B., and Zhao, B. (2022a). Drag reduction characteristics of bionic structure composed of grooves and mucous membrane acting on turbulent boundary layer. *J. Appl. Fluid Mech.* 15, 283–292. doi: 10.47176/jafm.15.01.32901

Zhang, X., Ma, J., Zheng, J., Dai, R., Wang, X., and Wang, Z. (2022b). Recent advances in nature-inspired antifouling membranes for water purification. *Chem. Eng. J.* 432, 134425. doi: 10.1016/j.cej.2021.134425

Zhao, Q., Yuan, D., Zhang, J., and Li, W. (2020). A review of secondary flow in inertial microfluidics. *Micromachines* 11, 461. doi: 10.3390/mi11050461